UNIVERSITY OF CALIFORNIA, SAN DIEGO

SAN DIEGO STATE UNIVERSITY

Reduced microstructural white matter integrity in a genetic metabolic disorder: A diffusion tensor MRI study

A dissertation submitted in partial satisfaction of the

requirements for the degree of Doctor of Philosophy

in

Clinical Psychology

by

Sunita Bava

Committee in charge:

University of California, San Diego

Professor Doris Trauner, Chair
Professor Natacha Akshoomoff
Professor Lawrence Frank
Professor Susan Tapert

San Diego State University

Professor Jörg Matt
Professor Sarah Mattson

2007

The Dissertation of Sunita Bava is approved, and it is acceptable in quality and form for publication on microfilm:

_____

_____

_____

_____

_____

_____
Chair

University of California, San Diego

San Diego State University

2007

Dedication

To my late father, Kishor Bava, who has inspired me from the beginning.

Table of Contents

List of Figures

List of Tables

Acknowledgements

I am especially grateful to my mentor, Dr. Doris Trauner, for her guidance and support throughout this project. Doris, you have encouraged independence from the beginning, and for that I am thankful. You are an exemplary clinician and scientist and it has truly been an honor to work with you.

I would also like to extend my sincerest thanks to Dr. Natacha Akshomoff, Dr. Lawrence Frank, Dr. Georg Matt, Dr. Sarah Mattson, and Dr. Susan Tapert for their valuable suggestions and for serving as committee members. Special thanks to Dr. Sandra Brown who encouraged this particular endeavor and to whom I am indebted for her mentorship throughout my training.

My sincere appreciation to the Pediatric Neurology Research Group, including Angela, Amy, Jenny, Lynne, Kirsten, Miriam, and Duc for their hard work and encouragement, whose vital contributions made this project possible. I also extend my warmest thanks to the cystinosis children and their families who so willingly participated in this study.

Special thanks to my friends and JDP classmates for the good times and for keeping me in touch with real life. A heartfelt thanks to my awesome family who have been there for me through and through. Thank you to my husband, Anup, for believing in me and for his love, encouragement, and support which have been instrumental in seeing this project through to completion. Thank you to my mother, Sharmila, a true woman warrior, for her love, sacrifice, and wisdom, to Dave for his constant support and exemplary attitude, and to my sister, Urvashi for always watching over me and for making me laugh the hardest. Thank you to my extended family, who have been

immensely supportive and whose endearing ways always remind me of what is important in life. Finally, to my father, whose story is the inspiration for this pursuit. You are in my heart always.

Curriculum Vitae

EDUCATION

2007 **Doctor of Philosophy in Clinical Psychology**
San Diego State University/University of California, San Diego
Joint Doctoral Program in Clinical Psychology

2004 **Master of Science in Clinical Psychology**
San Diego State University

2000 **Bachelor of Arts in Psychology,** minor in Cognitive Science
University of California, Los Angeles

RESEARCH EXPERIENCE

2001-2007 **Graduate Research Assistant,** Pediatric Neurology Research Group, UCSD Department of Neurosciences, San Diego, CA.
Supervisor: Doris Trauner, M.D.

2001-2003 **Graduate Research Assistant,** Project in Cognitive and Neural Development, UCSD Department of Cognitive Science, San Diego, CA.
Supervisors: Angela Ballantyne, Ph.D. and Doris Trauner, M.D.

2000-2001 **Research Assistant,** Functional Neuroimaging Core, UCLA Department of Psychology, Los Angeles, CA.
Supervisor: Tyrone Cannon, Ph.D.

1999-2000 **Stanley Scholar,** UCLA Department of Psychology**,** Los Angeles, CA.
Supervisors: Tyrone Cannon, Ph.D. and David Glahn, Ph.D.

CLINICAL EXPERIENCE

2006-2007 **Neuropsychology Intern,** UCLA Medical Psychology Assessment Center, Resnick Hospital and Semel Institute, Los Angeles, CA.
Supervisors: Robert Bilder, Ph.D., Susan Bookheimer, ,Ph.D., Jessica Horsfall., Roger Light., Ph.D., Jeff Schaeffer, Ph.D., Robert Tomasewski, Ph.D.

2005-2006 **Neuropsychology Trainee,** UCSD Child and Adolescent Inpatient Psychiatry Service, UCSD Medical Center, San Diego, CA.
Supervisor: Sandra Brown, Ph.D.

2004-2005 **Neuropsychology Trainee,** UCSD Outpatient Psychiatric Service, UCSD Medical Center, San Diego, CA.

Supervisor: Robert Heaton, Ph.D.

2004-2005 **Neuropsychology Trainee,** VASDHS Psychology Assessment Service, VA San Diego Healthcare System, San Diego, CA.
Supervisors: Dean Delis, Ph.D., Mark Bondi, Ph.D., Vince Filoteo, Ph.D.

2003-2004 **Psychology Trainee,** UCSD Child and Adolescent Inpatient Psychiatry Service, UCSD Medical Center, San Diego, CA.
Supervisors: Sandra Brown, Ph.D. and Susan Tapert, Ph.D.

2002-2003 **Psychotherapy Trainee,** SDSU Community Psychology Clinic, Department of Psychology, San Diego, CA.
Supervisors: Vanessa Malcarne, Ph.D. and Bina Parikh, Ph.D.

PUBLICATIONS

Glahn, DC, Kim, J, Cohen, MS, Poutanen, VP, Therman, S, Bava, S, Van Erp, TGM., Manninen, M, Huttunen, M, Lönnqvist, J, Standertskjöld-Nordenstam, CG, & Cannon, TD (2002). Maintenance and manipulation in spatial working memory: Dissociations in the prefrontal cortex. *Neuroimage, 17,* 201-213.

Zaidel, DW, Bava, S, & Reis V (2003). Relationship between facial asymmetry and judging trustworthiness in faces. *Laterality, 8,* 225-332.

Cannon, TD, Glahn, DC, Kim, J, Van Erp TGM, Cohen, MS, Nuechterlein, KH, Bava, S, & Shirinyan, D (2005). Dorsolateral prefrontal cortex activity during maintenance and manipulation of information in working memory in patients with schizophrenia. *Archives of General Psychiatry, 62(10),* 1071-1080.

Bava, S, Ballantyne, AO, & Trauner, DA (2005). Disparity of verbal and nonverbal IQ following early bilateral brain damage. *Cognitive and Behavioral Neurology, 18(3,)* 163-170.

Bava, S, Ballantyne, AO, May, SJ, & Trauner, DA (2005). Perceptual asymmetry for chimeric stimuli in children with early unilateral brain damage. *Brain and Cognition, 59(1),* 1-10.

Bava, S, Archibald, SA, & Trauner, DA (in press). Brain structure in prenatal stroke: Quantitative MRI analysis. *Journal of Child Neurology.*

Bava, S, Theilmann, RJ, Vu, D, Poehlmann, K, May, SJ, Sach, M, & Trauner, DA. (submitted). White matter integrity in a genetic metabolic disorder: A diffusion tensor MRI study.

Trauner, DA, Bava, S, Ballantyne AO, May, SJ, & Nichols, S. (submitted). Long-term neuropsychological outcome following neonatal stroke.

Published Abstracts

Bava, S, Theilmann, RJ, Trauner, DA (2006). Characterization of visuospatial impairment in a genetic metabolic disorder using diffusion tensor imaging. [abstract]. *Journal of the International Neuropsychological Society, 12(S1),* 80.

Sach, M, Vu, D, Bava, S, Dossick, D, Hillert, D & Trauner, DA (2006). Focal decreases in cerebral grey matter in a neurodevelopmental disorder assessed by voxel-based morphometry. [abstract]. Presented at the Organization for Human Brain Mapping Annual Conference, Florence, Italy.

Bava, S, Archibald, SL, Jernigan, TL, & Trauner, DA (2004). Quantitative MRI analysis of cerebral volume in children following early focal brain damage: Neurologic and cognitive correlates. [abstract]. *Journal of the International Neuropsychological Society, 10(S1),* 55.

Bava, S, Ballantyne, AO, & Trauner, DA (2002). Disparity of verbal and nonverbal ability following early bilateral brain damage. [abstract]. *Journal of Cognitive Neuroscience: Cognitive Neuroscience Society Supplement* (text omitted due to editorial error).

Bava, S, & Zaidel, DW (2001). Left-right facial asymmetry in social judgments. [abstract]. *Brain and Cognition, 48,* 229.

ABSTRACT OF THE DISSERATION

Reduced microstructural white matter integrity in a genetic metabolic disorder:

A diffusion tensor MRI study

by

Sunita Bava

Doctor of Philosophy in Clinical Psychology
University of California, San Diego,
San Diego State University, 2007

Professor Doris Trauner, Chair

Infantile nephropathic cystinosis is a genetic metabolic disorder in which cystine accumulates continuously in lysosomes, forming intracellular crystals throughout various organs in the body, including the kidneys, liver, thyroid, and brain. Cognitive deficits are particularly evident in the visuospatial domain and are accompanied by impairments in arithmetic and tactile recognition. Though the genetic causes and behavioral expression of this disorder are well characterized, the underlying neuropathological features are only grossly defined. The available literature suggests that cerebral white matter may be preferentially affected in this group, as cystine crystals have been identified in oligodendrocytes and perivascular macrophages. Within this context, the current study

used diffusion tensor MRI to investigate whether early processes in this disorder contribute to selective neuropathological changes. Accordingly, white matter integrity in the dorsal visual pathway (the "where" system) was examined in a young group (ages 3-7 years) of children with cystinosis (n = 24) and compared to an age-matched group of typically developing children (n = 24). A secondary aim of this study was to characterize the relationship between diffusion fractional anisotropy (FA), visuospatial functioning and white blood cell cystine level (an indicator of disease load).

Voxel-based analysis identified reduced FA primarily in bilateral inferior parietal white matter in children with cystinosis. Other areas bearing similar attenuations in anisotropy were found in the right mid-temporal and subgyral frontal regions. To expand this approach on a single-subject level, a region-of-interest (ROI) analysis was conducted focusing on parietal and temporal subregions, corresponding to the neuroanatomical visual pathways. In addition to changes in the inferior parietal lobule (IPL) as identified by voxel-level analysis, results of ROI analysis indicated bilaterally decreased FA in the superior parietal lobule (SPL). These findings occurred in the context of nonsignificant differences in FA in inferior temporal regions. A concomitant increase in the apparent diffusion coefficient (MD) in bilateral SPL and IPL was evident in the cystinosis group, with comparable MD values in inferior temporal white matter. Together, this pattern of findings is consistent with the hypothesized dissociation between the dorsal and ventral pathways in children with cystinosis.

Results of multiple regression analysis revealed an interaction between age and FA, which when decomposed into simple effects, indicated a stronger relationship between FA and visuospatial functioning for older cystinosis children. Specifically,

decremented performance on a task of visual-motor integration was associated with reduced FA in the right IPL in school-aged children with cystinosis (age > 5 years, n = 13, r = .74). Spearman correlations between white blood cell cystine level and MD in the right IPL (r = .46) and SPL (r = .50) were evident across the entire cystinosis group. In addition, correlations between cystine level and bilateral parietal MD became apparent in school-aged children, suggesting a progressive effect of cystine accumulation in addition to early white matter changes.

Taken together, significant attenuations in FA suggest that the genetic deletion underlying cystinosis results in early and regionally selective neuropathological changes which may involve myelin-forming oligodendroglia or their precursors. Contrary to expectations, relationships between anisotropy, cognitive performance, and cystine level, were only present in the older children of our group. These findings suggest that the accumulation of cystine over time may constitute a secondary progressive effect that interferes with white matter maturation. Moreover, the extent of cognitive deficit observed in children with cystinosis may result from an interaction of both the static and progressive processes in this condition.

I. Introduction

In the last decade, there have been considerable efforts to approach the study of neurodevelopmental disorders from a multidisciplinary perspective, merging evidence from neurobiology, cognitive science, and psychology. Developmental disorders with specific genetic etiologies provide a unique opportunity to integrate data from these related disciplines to better understand gene-brain-behavior relationships. Infantile nephropathic cystinosis is a rare genetic metabolic disorder well-suited for this type of multi-level modeling. At present, however, such a description is sorely lacking. This is particularly unfortunate, as the progressive nature of this condition represents a significant cause for morbidity and mortality in both children and adults. Cystinosis has widespread neurobiological effects, impacting both central and peripheral nervous system functioning. Cognitive deficits are evident, particularly in the visuospatial domain, and are accompanied by impairments in arithmetic and tactile recognition. While the genetic causes and behavioral expression of this disorder are generally well characterized, the underlying neuropathological features are only grossly defined. A description of the neuroanatomic correlates of this condition is thus warranted from both a theoretical and a clinical perspective and is prerequisite for an understanding of the linkage between the genetic, neurobiological, and behavioral components of this disorder.

A. Cystinosis

1. The Genetic Defect

Cystinosis is autosomal recessive in inheritance with an estimated incidence of 1 in 100,000 to 200,000 live births per year (Gahl, Thoene, & Schneider, 2002). The

genetic defect is one of cystine transport, wherein the accumulation of cystine within lysosomes occurs due to a deficiency in the lysosomal membrane transporter protein. As a result, cystine accumulates continuously in the lysosomes, forming intracellular crystals throughout the body. The progressive deposition of cystine crystals is a distinctive and diagnostic feature of cystinosis. The crystals are birefringent, hexagonal, or rectangular crystals and impair cellular energy metabolism, eventually inflicting widespread tissue and organ damage. Crystals been identified in various organs of the body including the kidneys, cornea, liver, bone marrow, thyroid gland, and brain (Gahl, 1986).

Cystinosis occurs due to mutations of the CTNS gene. The CTNS gene encodes the lysosomal membrane protein, cystinosin, which functions in cystine transport. In 1995, CTNS was mapped to chromosome 17p13 and later isolated to the deletion interval at locus D17S3829 (Gahl, 1995). Reportedly, more than 50 different mutations exist, the most common being a 57,257-bp deletion, which is found in approximately 50% of patients of northern European descent who have cystinosis (Touchman et al., 2000; Town et al., 1998). Patients with infantile nephropathic cystinosis have two severe mutations of CTNS. Two other subtypes of cystinosis, "intermediate" cystinosis and "ocular" cystinosis, have also been reported in the literature. Their genetic alteration is characterized by one severe CTNS mutation and one mild mutation, leaving some aspects of the transport function of cystinosin intact (Gahl, Thoene, & Schneider, 2002). The infantile subtype is the most common and the most devastating variant.

2. Diagnosis

The diagnosis of cystinosis is made by measuring leukocyte cystine content. Cystine levels in cystinosis are measured using specific assays involving cystine-binding proteins (Oshima, Willis, Furlong, & Schneider, 1974; Smith, Furlong, Greene, & Schneider, 1987). In normal individuals these preparations contain less that 0.2 nmol of half-cystine per milligram of protein, whereas in patients with nephropathic cystinosis, the values exceed 2.0 nmol of half-cystine per milligram of protein.

The mechanism by which cystine is toxic to tissues is not well understood. However, it is known that enzymatic activity may be altered by disulfides such as cystine. It is possible that cystine may act as a thioenzyme and modify cell function. Pyruvate kinase (PK) is a thiolic enzyme that is necessary for the glycolytic pathway, the main route that provides energy for brain function. Disulfides like cystine can alter thiolic enzymes. Feksa et al. (2004) investigated the effects of cystine on PK activity in the cortex of developing Wistar rats. The effect of a cystine-depleting agent, cysteamine, on enzyme activity was also examined. Findings revealed an inhibition of PK activity by cystine, suggesting possible cytotoxic effects of cystine on brain tissue.

3. Clinical Manifestations and Treatment

Infantile nephropathic cystinosis presents within the first year of life with failure to thrive and renal tubular dysfunction (Fanconi syndrome). Progression of renal disease results in renal failure within the first decade of life. In addition, metabolic conditions associated with this disorder can present in the form of electrolyte imbalances, growth retardation, hypothyroidism (Gahl, Schneider, Thoene, & Chesney, 1986), or

hypophosphatemic rickets (Schneider, Katz, & Melles, 1990). Late effects such as retinal blindness and photophobia (Kaiser-Kupfer, Caruso, Minkler, & Gahl, 1986), progressive distal myopathy with muscle wasting (Charnas et al., 1994; Gahl et al., 1988), pulmonary dysfunction (Anikster et al., 2001), diabetes mellitus (Fivush et al., 1987), and central nervous system deterioration (Ehrich, Stoeppler, Offner, & Brodehl, 1979; Fink et al., 1989) have been documented as well.

The development of a cystine-depleting agent, cysteamine, has dramatically improved the prognosis of individuals with cystinosis. The mechanism of this agent involves the entry of cysteamine into the lysosomal membrane, where it reacts with cystine to form the mixed disulfide, cysteamine-cysteine, which then leaves the cystinotic lysosome by means of an intact lysine transporter (Gahl, Thoene, & Schneider, 2001; Pisoni, Thoene, & Christensen, 1985). Since the introduction of cysteamine in the 1980s, children with cystinosis have experienced improvement in growth and increased protection of renal function (Gahl et al., 1987; Markello, Bernardini, & Gahl, 1993). Although cysteamine does not restore renal tubular function, it is effective in blunting the progression of renal dysfunction. Still, eventual renal transplantation is typically necessary. In addition to continuous cysteamine treatment, supportive therapy is needed to replenish the loss of fluids and solutes that results from impaired renal tubular reabsorption. Supplements are often required to replace wasted nutrients and unrestricted intake of water and salt is important for preventing dehydration (Gahl, Thoene, & Schneider, 2002).

The advent of renal transplantation procedures and cysteamine therapy has allowed individuals with infantile nephropathic cystinosis to survive well into adult life.

With the increase in life expectancy more severe neurological and cognitive problems have surfaced and currently constitute the most significant complications of this condition.

4. Neuroanatomical Findings

Postmortem studies of patients with cystinosis have identified a number of neuropathological abnormalities. These include cystine crystal deposition in the deep white matter and periventricular white matter, choroid plexus, meninges, basal ganglia, anterior pituitary, and internal capsule (Ebbesen, Mygind, & Holck, 1976; Jonas et al., 1987; Levine & Paparo, 1982; Vogel et al., 1990). Although cystine crystals have been identified in the cytoplasm of several cell types, they appear to be most common within pericytes, and in parenchymal cells of the white matter and cell processes extending through the white matter (Vogel et al., 1990). Hydrocephalus (Ehrich, Stoeppler, Offner, & Brodehl, 1979; Ross, Strife, Towbin, & Bove, 1982), demyelination, and vacuolar, necrotic, and spongiform changes have also been reported in cystinosis. Neuroimaging studies show additional evidence of ventricular dilatation and cortical and white matter atrophy (Broyer, Tete, & Gubler, 1987; Cochat, Drachman, Gagnadoux, Pariente, & Broyer, 1986; Fink et al., 1989; Hodge, Hesselink, & Trauner, 1992; Nichols, Press, Schneider, & Trauner, 1990; Wolff, Ehrich, Offner, & Brodehl, 1982).

Nichols, Press, Schneider, and Trauner (1990) demonstrated evidence of cortical atrophy in children with cystinosis based on clinical neuroradiological readings of MRI scans. Of this group, 64% had moderate to severe atrophy, and 27% had mild atrophy. A general frontal predominance was found, in agreement with a previous study

documenting frontal cortical atrophy secondary to white matter atrophic changes (Vogel et al., 1990). In Nichols et al. (1990), atrophy was inversely related to cognitive performance, particularly on a test of visual short-term memory (Stanford-Binet Bead Memory subtest). Visual short-term memory was more than one standard deviation below the mean in the group with moderate to severe atrophy, whereas auditory short-term memory (Stanford-Binet Memory for Sentences subtest) was within the average range, suggesting a dissociation between visual and auditory memory.

A follow-up study including a larger group of participants found structural abnormalities in two-thirds of individuals with cystinosis (age range: 2 to 21 years) (Trauner, Williams, Hesselink, & Schneider) . Of these, approximately 60% had central volume loss, 57% had cortical volume loss, and 86% had white matter abnormalities consistent with incomplete or deficient myelination or partial demyelination. The areas of deficient myelination were either diffuse or primarily in peri-atrial regions and were bilateral. Eighty-six percent also showed signal hyperintensities in subcortical regions. When these findings were interpreted along with participants' performances on neuropsychological measures, children with abnormal MRIs scored significantly lower than did the children with normal MRIs on a test of extrapersonal orientation. There was also a trend toward worse performances on a test of spatial memory. In contrast, Full Scale IQ and performances on visual perceptual tests, including visual form discrimination and incomplete figures were comparable between the normal MRI and abnormal MRI groups.

Quantitative volumetric MRI analysis of 12 individuals with cystinosis (age range: 7 to 30 years) was conducted in comparison to age and gender matched controls.

In subcortical regions, the anterior diencephalon, primarily the hypothalamus, was larger in the cystinosis group and the thalamic region was significantly smaller relative to controls. Sulcal fluid volume was significantly increased in the cystinosis group, but ventricular volume was comparable. The limbic lobe was not different between the two groups, but a measure of the remaining cortex was significantly reduced in the cystinosis group. Specific regions that showed volume differences included the orbitofrontal, inferior parietal, and superior parietal regions, which were reduced relative to controls (unpublished data).

The pathogenesis of neuroanatomical alterations in cystinosis is presently unknown. It is possible that structural alterations are due to the continuous accumulation of cystine. The transport of cystine into cells of the brain is essential for the supply of cystine for glutathione synthesis. The cystine-glutamate transport system facilitates the uptake of cystine with concomitant release of glutamate (Kleta et al., 2004). One mechanism of structural damage is that an excess of extracellular cystine might cause the release of glutamate from glial cells, inducing excitoxicity. While this may underlie the brain damage observed in cystinosis, it is also possible that alterations in structure are present early in development, emerging from aberrations in cellular components and membranous organelles that are directly related to the CTNS gene.

5. Neurological Complications

Neurological complications associated with cystinosis include early motor delays and cognitive dysfunction that are apparent in childhood (Trauner, Chase, Scheller, Katz, & Schneider, 1988) as well as late-onset encephalopathy that occurs in young adults.

Specific neurological deficits that have been identified in children with cystinosis include oral-motor dysfunction, diffuse hypotonia, gross and fine motor delays, and in some cases intention tremor (Broyer, Tete, & Gubler, 1987; Cochat, Drachman, Gagnadoux, Pariente, & Broyer, 1986; Ross, Strife, Towbin, & Bove, 1982). The impairments are generally mild with no major associated functional disabilities. However, there are a significant number of young adults between the ages of 18-24 who display a progressive myopathy with severe oral-motor weakness, dysphagia, dysphonia, and distal wasting of hand muscles (unpublished data). The cause of the myopathy remains unclear as does the relationship between early motor delays and the later development of myopathy.

As individuals with cystinosis reach adult life, they may develop a progressive neurologic disorder, described as "cystinosis encephalopathy," in which motor and mental declines occur, with dementia resulting (Broyer et al., 1996). Although the cause of this progressive condition is presently unknown, it is suggested that the accumulation of cystine in brain parenchyma might account for the encephalopathy.

6. Cognitive features

Children with cystinosis demonstrate intellectual functioning within the average range (Ehrich et al., 1979; Trauner, Chase, Scheller, Katz, & Schneider, 1988; Williams, Schneider, & Trauner, 1994; Wolff, Ehrich, Offner, & Brodehl, 1982; Spilkin, Ballantyne, Babchuck, & Trauner, 2007); however, there is evidence that IQs of children with cystinosis are lower than what would be expected based on comparison with their siblings and parents (Williams, Schneider, & Trauner, 1994). Specific cognitive deficits that have been identified in adults and children with cystinosis include impaired visual

memory (Nichols, Press, Schneider, & Trauner, 1990; Trauner, Chase, Scheller, Katz, & Schneider, 1988), visuospatial function (Ballantyne & Trauner, 2000; Scarvie, Ballantyne, & Trauner, 1996; Wolff, Ehrich, Offner, & Brodehl, 1982), tactile recognition (Colah & Trauner, 1997), and arithmetic ability (Ballantyne, Scarvie, & Trauner, 1997). Deficits in the visual domain appear to be isolated to the spatial component of visual function, as visual perceptual functions are largely intact (Ballantyne & Trauner, 2000; Trauner, Spilkin, Williams, & Babchuck, 2007).

Evidence for a specific cognitive impairment in cystinosis as opposed to a nonspecific effect of chronic renal failure on neurocognitive functioning was demonstrated by Trauner, Chase, and Ballantyne (1989). When compared to chronic renal controls, children with cystinosis showed average general intellectual functioning but poor visual memory, whereas the former group demonstrated a global impairment in intellectual functioning, with no specific impairment. These findings lend support to a condition specific deficit in cystinosis that is beyond what can be accounted for by the effects of renal failure.

In a study of academic performance in children and young adults with cystinosis using the Wide Range Achievement Test – Revised (Ballantyne, Scarvie, & Trauner, 1997), children with cystinosis performed within the average range on tests of reading and spelling, but in the low average range on arithmetic. Although as a group cystinosis children performed in the average range in spelling, there was a trend toward poorer performance on the spelling subtest. There was no evidence of a developmental lag or a deterioration of function with age. In addition, poor performances did not appear to be due to delayed learning of academic skills, as the standard scores of the children and

young adults were similar. Because both arithmetic and spelling require integration of visual skills, weaknesses in these areas may be the result of deficits in certain aspects of visual processing.

Colah and Trauner (1997) assessed sensory processing in children and adults with cystinosis using a task of tactile recognition of common objects. The cystinosis group performed significantly worse in identifying objects than did controls. Moreover, participants over 7 years of age demonstrated prolonged response times to correctly identify objects. Given their intact sensory functions, these children appear to have deficits in mental imaging ability and may have difficulty with speeded information processing as well.

In another study, Scarvie, Ballantyne, and Trauner (1996) studied the performance of children with cystinosis on the Beery Test of Visual Motor Integration (VMI) in comparison to that of controls. The cystinosis group demonstrated a significantly worse performance than age and gender matched controls. There was a tendency for the cystinosis group to make rotation and relative size errors. Further analysis of findings suggested that for older children with cystinosis, their visuomotor skills tended to fall farther below what would be expected of their chronological age. Given this pattern, it is possible that either the accumulation of cystine over time or another undefined cumulative effect of the metabolic disorder on the central nervous system may account for the increasing gap between expected and actual performance.

Based on findings from previous studies, Ballantyne and Trauner (2000) aimed to better characterize the nature of the processing deficits in children with cystinosis using tests of visuospatial and visuoperceptual functioning. Compared with control subjects,

cystinosis subjects showed impairments on each of the spatial measures, involving extrapersonal orientation, mental rotation, and short-term memory of spatial location. Spatial processing deficits were evident even after partialling out the effect of IQ on spatial test scores. Most striking was that impaired spatial processing occurred in the context of intact perceptual processing. The results supported the hypothesis of a dissociation in visual processing and suggested that there may be a differential effect of cystinosis on the two visual processing streams of the central nervous system, such that the "where" pathway (i.e., posterior parietal) may be affected to a greater extent than the "what" pathway (i.e., inferior temporal).

Another study by Schatz (2002) examined the performance of children with cystinosis on verbal and visual learning tests. Findings revealed a dissociation between visual and verbal learning, in that the cystinosis group performed at a significantly lower level than controls on almost all indices of visual learning and memory, while no differences were found between the groups on verbal learning indices. A related study demonstrated that in the cystinosis group, increasing stimulus exposure time (from one to three seconds) resulted in an improvement in visual learning, with performances comparable to control children who had a one second exposure time. Findings from this study suggest that decreasing the demands on processing speed may enhance the performance of children with cystinosis in the domain of visual learning and memory.

Extending upon current findings of visuospatial processing deficits in children with cystinosis, Spilkin et al. (2007) administered tasks of executive functioning to individuals with cystinosis (ages 8-34 years) to understand the impact of processing deficits on more demanding cognitive tasks. Findings demonstrated a higher rate of

impairment on tasks of visuospatial executive skills including design fluency, spatial planning, and complex visual-motor sequencing. Further examination is needed to determine whether executive deficits constitute another component of cognitive weaknesses in children with cystinosis or whether visuospatial processing deficits are responsible for diminutions in executive functioning.

As mentioned earlier, cystine accumulation in the brain over time may be related to neuropathological and cognitive consequences. There is also the possibility that cysteamine treatment may adversely affect brain and cognitive function. Although the effects of cysteamine on the brain are unclear, cysteamine has been reported to inhibit somatostatin in brain tissue (Papachristou, Liu, & Patel, 1994). A study by Broyer et al. (1996) showed improvement in cystinosis related encephalopathy after administration of cysteamine for several months. To assess the effects that treatment of cystinosis with cysteamine might have on cognitive functions, children with (≥ 6 months) and without cysteamine treatment were compared on measures of IQ, visual memory, visual motor, visual perceptual, and visual spatial tasks. Although no differences were found between the groups on any of the above indices, there was a trend toward better performance in children who were being treated with cysteamine (unpublished data).

7. Behavioral Studies

Delgado, Schatz, Nichols, Appelbaum, and Trauner (2005) examined the behavioral profiles of children and adolescents with cystinosis using parents' responses to the Achenbach Child Behavior Checklist (CBCL). Responses were compared to those provided by parents of typically developing children and to parents of children with

cystic fibrosis who served as a chronic disease control group. Parents of children with cystinosis endorsed greater problems for aspects of their child's behavior, including somatic complaints, social problems, and attention problems. These findings were significant when compared to controls and to the cystic fibrosis group. Nonetheless, the mean scores for all groups were within the normal range, but the cystinosis group had a significantly higher percentage of elevated scores on the social problems scale compared to the other two groups.

In sum, previous studies have shown that children with cystinosis have a number of cognitive problems, including impairments in visual spatial function (Ballantyne & Trauner, 2000), visual memory (Nichols, Press, Schneider, & Trauner, 1990; Trauner, Chase, & Ballantyne, 1989), and tactile recognition (Colah & Trauner, 1997) as well as academic difficulty, particularly in arithmetic (Ballantyne, Scarvie, & Trauner, 1997). In addition, social and attentional problems have also been identified as behavioral weaknesses in this group (Delgado, Schatz, Nichols, Appelbaum, & Trauner, 2005). The cognitive and behavioral phenotype of infantile nephropathic cystinosis continues to be studied in greater depth with aims to generate gene-brain-behavior models that will inform treatment and intervention. Currently, however, a description of the integrity of neuroanatomical pathways is lacking, as is an illustration of how disintegrated pathways are related to cognitive functioning and to metabolic processes. This characterization is critical for model generation and is the basis of the current study.

B. Diffusion tensor imaging (DTI)

Molecular diffusion refers to the random movement of water molecules, termed Brownian motion that occurs as a result of the molecules' thermal properties. While the average displacement of water molecules is on the order of 10μm in 50 seconds, the displacements are nonetheless measurable by nuclear magnetic resonance (NMR) imaging. Diffusion tensor imaging exploits the molecular diffusion effects in the NMR signal by using bipolar magnetic field gradient pulses (Stejskal & Tanner, 1965). Diffusing water in the presence of magnetic field gradients causes a loss in the MRI signal that is proportional to the local tissue diffusion. By careful manipulation of special "diffusion weighting gradients" applied in addition to the normal magnetic gradients, an MR image with signal changes due to local diffusion can be created.

When the patient enters the bore of the MRI scanner, the nuclear spins are lined up along the direction of the large magnet. A small field that rises linearly in space, called a gradient, produces a spatial variation in the resonant frequency that is used to produce the MR image. Magnetic field gradients of certain duration are applied to add a smaller magnetic field to spins located in different regions within the tissue. By applying another gradient pulse at a later time, information is obtained about how much the spins have spread (diffused) during this time. Because the brain is filled with cells of different concentrations and in different compartments, water will diffuse at different rates depending on the structural makeup of the brain tissue. In highly structured tissues such as white matter fiber tracts, water molecules move anisotropically due to restriction by membranous elements, whereas in gray matter there is a greater tendency toward diffusion in each direction. Diffusivity is a measurement of the magnitude of diffusional

motion and anisotropy is a measurement of the directional variance of the motion (Moritani, Ekholm, & Westesson, 2004).

With simple diffusion MRI, diffusion can be described using a single (scalar) parameter, the diffusion coefficient, D. The effect of diffusion on the NMR signal is an attenuation (A), which depends on D and the b-value, which characterizes the amplitude, width, and separation in time between the bipolar pulses.

$$A = \exp(-bD)$$

In the presence of anisotropy, diffusion cannot be characterized by a single scalar coefficient, but requires a tensor, **D**, which describes molecular mobility along each direction and the correlation between these directions. The tensor is expressed as the following symmetric matrix:

$$\mathbf{D}_{eff} = \begin{bmatrix} D_{xx}^{eff} & D_{xy}^{eff} & D_{xz}^{eff} \\ D_{yx}^{eff} & D_{yy}^{eff} & D_{yz}^{eff} \\ D_{zx}^{eff} & D_{zy}^{eff} & D_{zz}^{eff} \end{bmatrix}$$

To determine the diffusion tensor, diffusion-weighted images must be collected along several gradient directions. As the diffusion tensor is a 3x3 symmetric matrix, it has 6 independent parameters. Thus, measurements along at least six directions is required, along with an image acquired without diffusion weighting (b = 0). This minimal set of images may be repeated for averaging to increase signal-to-noise ratio (Basser, Mattiello, & LeBihan, 1994a, 1994b). From the components of the diffusion tensor, one can calculate indices that reflect either the average diffusion or the degree of anisotropy in each voxel. One can also determine the main direction of diffusivities in each voxel and the diffusion values associated with these directions. This is given by the eigenvectors and the eigenvalues of the diffusion tensor (Le Bihan et al., 2001).

Tensor data is described best using the concept of diffusion ellipsoids. An ellipsoid is a three-dimensional representation of the diffusion distance covered in space by molecules in a given diffusion time. These ellipsoids can be displayed for each voxel and are calculated from the eigenvalues, λ_1, λ_2, and λ_3, which correspond to D_{xx}, D_{yy}, and D_{zz} (see Figure 1). The main axis of the ellipsoid gives the main direction of diffusion in the voxel, which coincides with the direction of the fibers. The eccentricity of the ellipsoid provides information about the degree of anisotropy and its symmetry. Isotropic diffusion would be seen as a sphere, whereas anisotropic diffusion may be seen as cigar- or disc-shaped. The eigenvalues, or principal diffusivities, of the diffusion tensor characterize the magnitude or rate of water diffusion along each of the three principal axes of the diffusion tensor ellipsoid, and are given in mm^2/s. The direction of the three principal axes in three-dimensional space is given by the eigenvectors. In the simple Gaussian model of diffusion the principal eigenvector can be interpreted as the main fiber direction.

In summary, diffusion tensor MRI is a technique that provides information about white matter microstrucure *in vivo*. Data derived from DTI can be analyzed in three ways to extract information on tissue microstructure for each voxel. The mean diffusivity, which characterizes the overall mean-squared displacement of molecules (average ellipsoid size) and the overall presence of obstacles to diffusion; the degree of anisotropy, which describes how much molecular displacements vary in space (ellipsoid eccentricity) and is related to the presence of oriented structures; and the main direction of diffusivities (main ellipsoid axes), which is linked to the orientation in space of these structures (Le Bihan et al., 2001).

1. The Contribution of Myelin to Anisotropy

Myelin is a spiral membranous structure that is tightly wrapped around axons. The myelin sheath is constructed from layers or lamellae and is a system of condensed plasma membranes with alternating protein-lipid-protein-lipid lamellae as the repeating subunit. Myelination starts in the brain in the 30th gestational week. The main period of myelination is thought to be terminated by 2 years of age (Brody, Kinney, Kloman, & Gilles, 1987), although the process is reported to continue until early adulthood. White matter increases its overall volume and becomes more myelinated in a region-specific fashion (Paus et al., 2001), following a posterior–anterior progression with development (van der Knaap & Valk, 1995).

The temporal order in which different brain structures first acquire a "myelinated" appearance has been demonstrated in histological studies of fetal and infant development (Keene & Hewer, 1931; Yakovlev & Lecours, 1967). Projection fibers develop first, followed by the commissural and finally association fibers. Myelination is first observed in the pons and cerebellar peduncles (birth); followed by the posterior limb of the internal capsule, optic radiations and the splenium of the corpus callosum (1–3 months); the anterior limb of the internal capsule and the genu of the corpus callosum (6 months); and finally the white matter of the frontal, parietal and occipital lobes (8–12 months) (Hittmair et al., 1994; Mukherjee et al., 2001; Paus et al., 2001; Stephanova, 2001; Thomas et al., 2000).

Premyelination steps such as the formation and maturation of oligodendrocytes are prerequisites of normal myelination (Thomas et al., 2000). This process evolves in

three phases. First, formation of irregular processes (the so-called ‘‘initiator processes’’) with predominant radial orientation that serve as identifiers of targeting axons. This is followed by spiral

ensheathment of the axon which starts with an extension of an initiator process that elongates and wraps around, forming the first turn of the myelin sheath. Finally, nodes of Ranvier are formed to interrupt the myelin sheath, allowing the surface of the axon to communicate directly with the interstitial fluid. The longitudinal spacing of myelin sheaths and nodes of Ranvier is controlled by the axons. Similarly, the number of myelin lamellae formed by a single oligodendrocyte is also specified by the axon (Baumann & Pham-Dinh, 2001; Butt & Berry, 2000; Hardy & Friedrich, 1996).

Myelination leads to tissue compaction, which restricts the motility of water molecules. However, increases in anisotropy during development appear to take place even before the histologic appearance of myelin (Prayer et al., 2001; Schmithorst, Wilke, Dardzinski, & Holland, 2002; Wimberger et al., 1995). This increase has been attributed to microstructural changes occurring during the premyelination period. During this period there is an increase in the number of microtubule-associated proteins in axons, an increase in axon diameter, formation of the axolemmal membrane and transmembrane bulbs, and wrapping of axons by oligodendrocyte processes (Filippi et al., 2003). It is also associated with changes in the axonal membrane such as an increase in conduction velocity and changes in Na+/K+ -ATPase activity.

During the myelination period itself it appears that greater anisotropy is the result of hindrance to water diffusion by axonal membranes and layering of myelin sheaths (Beaulieu & Allen, 1994). The increase in white matter anisotropy takes place at different

rates for different brain areas, as does myelination. While myelination accounts for some aspects of anisotropic change, other factors are also contributory. These include the density of fibers, the average fiber diameter, and the directional similarity of the fibers in a voxel (Mamata et al., 2002; Shimony et al., 1999; Virta, Barnett, & Pierpaoli, 1999). Diffusion anisotropy will be present under any circumstance in which the cytoarchitecture of the tissue is arranged in such a way as to lead to greater hindrance of water motion in one direction as compared with others (Le Bihan et al., 2001; Pierpaoli & Basser, 1996).

The mechanism by which myelin may be affected in cystinosis is presently unknown. As observed in another lysosomal storage disease, metachromatic leukodystrophy, it is possible that the accumulation of cystine in the oligodendroglial lysosomes may result in lysosomal degeneration which can then cause a release of toxic enzymes into the cell cytoplasm and cause reactions that lead to cell death (Gieselmann, Polten, Kreysing, & von Figura, 1994; van der Knaap, Breiter, Naidu, Hart, & Valk, 1999). In this way, intracellular crystal formation may simulate cytotoxic edema, as occurs in glial cells, axons, and myelin sheaths. Membrane damage may instigate a cascade of events that may eventually result in loss of fiber integrity. Given that each oligodendrocyte contributes myelin to several axons, more widespread abnormalities may be apparent and attributed to pathology at the level of the glia.

2. Diffusion Tensor Imaging in Children

The normal brain of neonates and infants has significantly higher diffusivity and lower anisotropy values than the adult human brain (Neil et al., 1998). This is due to the

high water content of the infant brain and fewer myelinated fibers as compared to adults. With typical development, mean diffusivity (MD) has been found to decrease and anisotropy to increase (Huppi et al., 1998; Neil, Miller, Mukherjee, & Huppi, 2002; Schmithorst, Wilke, Dardzinski, & Holland, 2002). By the age of 2 years, MD and anisotropy values resemble those measured in adults (Huppi et al., 1998; Morriss, Zimmerman, Bilaniuk, Hunter, & Haselgrove, 1999; Nomura et al., 1994; Sakuma et al., 1991).

Diffusivity values decrease with increasing age in a monotonic fashion during development until they reach adult values (Mukherjee et al., 2001). Averaged diffusion maps of the pediatric brain show contrast between white and gray matter, with the MD values for white matter being higher than those for gray matter. This contrast gradually diminishes and is undetectable by 7 years of age. Some of the decrease in MD is attributable to decreasing brain water content with development; however, Partridge et al. (2004) point out that the percent decrease in MD over age is substantially greater than would be expected from the actual percent decline in brain water content during the same range of time. Thus, decreases in MD appear to reflect more processes than water loss, including changes in the microenvironment in response to myelination.

Several studies have demonstrated a significant positive correlation of fractional anisotropy (FA), a measure of the fraction of the magnitude of the diffusion tensor attributable to anisotropic diffusion, with age. In a study of brain development in children (5 -18 years), Schmithorst, Wilke, Dardzinski, and Holland (2002) identified specific regions showing significant increases in FA with age. These included the internal capsule, corticospinal tract, left arcuate fasciculus, and right inferior longitudinal

fasciculus. Anisotropy values were highest in the internal capsule, which in addition to the fiber tracts projecting through it also showed the strongest correlation with age. As these are fibers of the primary and supplementary motor areas, the strong correlation appears consistent with the maturation of these regions for motor control. The inferior longitudinal fasciculus, which also demonstrated a strong correlation with age, consists of fiber tracts connecting occipital and temporal areas and has been implicated in visual recognition and visual memory. The arcuate fasciculus, a band of fibers connecting the primary language areas known as Broca's and Wernicke's area showed a significant increase in FA in the left hemisphere only, which coincides with typical language development. Areas in which MD negatively correlated with age were distributed throughout the white matter.

Snook, Paulson, Roy, Phillips, and Beaulieu (2005) studied regional changes in brain development using DTI in a group of school-aged children (8-12 years) and young adults (21-27 years). Regions included the major white matter tracts, subcortical white matter regions, cortical gray matter, and deep gray matter structures. Fractional anisotropy was greatest in the splenium of the corpus callosum, followed by the genu of the corpus callosum, the posterior limb of the internal capsule, the anterior limb of the internal capsule, the corona radiata, the external capsule and centrum semiovale, and the subcortical white matter regions. Within gray matter, anisotropy was highest in the thalamus, followed by the globus pallidus, cortical gray matter, caudate, and finally, the putamen. This pattern of anisotropy values was similar to that of adults. Although a cross-sectional comparison, significant differences in anisotropy between the younger and older age groups were evident in the splenium and genu of the corpus callosum, the

corona radiata, the putamen, and the head of the caudate nucleus. Significant decreases in MD were seen in 9 of 13 brain regions in children over the 5-year age span, with the exception of the genu of the corpus callosum, posterior limb of the internal capsule, thalamus, and cortical gray matter.

Schmithorst, Wilke, Dardzinski, and Holland (2005) studied the relationship between cognitive abilities and white matter structure as assessed with DTI in children ages 5 to 18. Fractional anisotropy in the left parietal and right frontal regions appeared to correlate most with Wechsler Full Scale IQ (.51; .46) and Verbal IQ (.57; .48). The right occipito-parietal (.41) and occipito-temporo-parietal regions (.41) correlated most highly with Performance IQ. Mean diffusivity was not found to correlate with IQ indices. Given that the basic processes involved in white matter maturation are increases in the density of fiber tracts, resulting in more directionally restricted extracellular space and changes in the intracellular compartment including a greater concentration of membranous elements, the process affecting extracellular space should lead to an increase in anisotropy and a decrease in diffusivity, due to restricted diffusion perpendicular to the axon direction. The intracellular process should lead only to a decrease in diffusivity. Given that strong FA-IQ correlations were found in the absence of MD-IQ correlations, cognitive ability appears to reflect fiber organization and/or density. Together with the results of Schmithorst, Wilke, Dardzinski, and Holland (2002) who found regionally specific increases in FA, findings suggest that efficient organization of white matter association fibers is essential for optimal cognitive performance.

Barnea-Goraly et al. (2005) examined developmental changes in white matter FA in typically developing children and adolescents between 6 and 19 years of age. Findings were consistent with previous studies that have reported age-related increases in white matter anisotropy in the arcuate fasciculus, in motor areas, and in the internal capsule (Paus et al., 2001; Schmithorst, Wilke, Dardzinski, & Holland, 2005). In addition, the study replicated, in a larger sample, age-related FA increases in prefrontal regions (Klingberg, Vaidya, Gabrieli, Moseley, & Hedehus, 1999).

According to Filippi et al. (2003), alterations in anisotropy may be related to the disruption in any of the processes that characterize myelin maturation. Increased or abnormal amounts of intraaxonal water may be caused by aberrant microtubule or microfilament production, leading to increased diffusivity and decreased anisotropy. Increased extracellular water volume may be due to hypomyelination, poor glial processing, or decreased synaptic density and can lead to the same outcome. Abnormal axonal growth can lead to diminished axonal diameter and result in persistently abnormal anisotropy.

Thomalla et al. (2004) suggest that loss of axonal structures may result in less restricted diffusion perpendicular to the main direction of fibers and consequently elevated λ_2 and λ_3. In addition, membrane disintegration and cellular debris creates new diffusion barriers that lead to a decrease in diffusivity parallel to the main fiber direction and reduced λ_1. In combination, these effects can result in a reduction in anisotropy, while the effect on averaged diffusion indices might remain unchanged.

Eigenvalue analysis has shown a reduction of diffusion perpendicular to the fiber tracts (λ_2 and λ_3) whereas diffusion parallel to the tracts (λ_1) remains fairly constant with

maturation (Klingberg, Vaidya, Gabrieli, Moseley, & Hedehus, 1999; Partridge et al., 2004; Snook, Paulson, Roy, Phillips, & Beaulieu, 2005; Suzuki, Matsuzawa, Kwee, & Nakada, 2003; Thomalla et al., 2004). Hence, increases in FA do not appear to result from an increase in the parallel eigenvalue, but rather by a decrease in the perpendicular eigenvalues. This observation provides evidence that anisotropy results from more than just a decrease in water content, as reduction in water should result in decreased water motion in all directions. A greater reduction in the two perpendicular eigenvalues has been observed with maturation (between children of 1–10 years and young adults) in the frontal and parietal lobe white matter (Suzuki, Matsuzawa, Kwee, & Nakada, 2003) as well as in the basal ganglia, internal capsule, and corpus callosum in children aged 31 gestational weeks to 11 years, with the majority of the change occurring in the first 2 years of life (Mukherjee et al., 2001). Separating changes in water content form changes in myelination is an area of continued studied. Evidence thus far, suggests that age-dependent reduction in the minor eigenvalues may be reflective of myelination and that changes in the major eigenvalue (λ_1) may be more suggestive of changes in water content (Mukherjee et al., 2002).

C. The "What" and "Where" of Visual Processing

Both animal and human research provide strong evidence for the existence of two anatomically and functionally distinct visual processing systems originating from the occipital cortex. Ungerleider and Mishkin (1982) located the two visual systems within the primate visual cortex. The occipitoparietal system follows a dorsal path to the parietal lobe and the occiptotemporal system follows a ventral path to the temporal lobe.

The dorsal pathway is proposed to subserve spatial processing, including analysis of spatial relationships and location as well as navigational abilities, and is referred to as the "where" pathway. The ventral pathway is proposed to specialize in perceptual processing related to object identification and discrimination, and is referred to as the "what" pathway (DeYoe & Van Essen, 1988; Haxby et al., 1994; Ungerleider & Haxby, 1994). The two streams then project to the frontal cortex via different pathways (Boussaoud, di Pellegrino, & Wise, 1995).

A double dissociation between these visual processing streams was demonstrated using selective lesion analysis (Ungerleider & Mishkin, 1982). Lesions of the posterior parietal cortex were shown to result in spatial processing deficits, but intact perceptual abilities, whereas lesions of the inferior temporal cortex were associated with visuoperceptual impairments, but preserved spatial abilities. More recent work has depicted this dissociation utilizing in vivo techniques (Courtney, Ungerleider, Keil, & Haxby, 1996; James, Culham, Humphrey, Milner, & Goodale, 2003; James, Humphrey, Gati, Menon, & Goodale, 2002). Using varied perceptual and spatial tasks, several studies have described the distributed network of brain regions involved in these processes.

An fMRI study conducted by Aguirre and D'Esposito (1997) revealed increased activation in the fusiform gyrus, parahippocampus, lingual gyrus, and occipital gyrus in response to a perceptual task. In contrast, activation was apparent in the inferior parietal, precuneus, superior parietal, superior frontal, and premotor cortex in response to a location task. Rao, Zhou, Zhuo, Fan, and Chen (2003) studied the activation patterns in the two visual processing pathways in response to an integrated visuospatial task in

which form discrimination and spatial location were combined. The fMRI data demonstrated that the task activated both ventral (the inferior temporal gyrus and the fusiform gyrus) and dorsal (the angular gyrus and precuneus) brain regions. Shen, Hu, Yacoub, and Ugurbil (1999) demonstrated that spatial recognition was associated with predominant activation in the right hemisphere. Specifically, these areas included the right fusiform gyrus, the bilateral superior parietal lobule, right superior occipital cortex, right lateral precentral cortex, right superior frontal sulcus, right postcentral sulcus, left frontal pole, and anterior cingulated gyrus. Compared to the spatial task a visual form recognition task activated greater left hemisphere structures including the cingulate cortex and cerebellum in addition to the traditional inferior ventral regions.

Goodale and Milner (1992) offer an alternative view to the two processing streams proposed by Ungerleider and Mishkin (1982). Whereas Ungerleider and Mishkin's model focuses on the input system, Goodale and Milner (1992) focus on the way visual information is processed and transformed for output. They propose a "how" versus "what" model, wherein the dorsal pathway is proposed to engage in action-relevant (egocentric) visual processing and the ventral pathway to engage in perceptual processing independent of a particular viewpoint. This revision of the original two-system model was based on lesion analysis were lesions of the inferior temporal area resulted in visual agnosia and lesions in the posterior parietal cortex resulted in optic ataxia. The revised model suggests that spatial processing can occur in either stream depending on the output characteristics. Thus, the functional significance of the dorsal pathway is proposed to be the "vision for action" stream and ventral stream to be the "vision for perception" stream.

Much work has been dedicated to parsing the components of spatial processing and identifying their anatomical bases. Studies of mental rotation have localized this skill to the right parietal area (Ditunno & Mann, 1990), while others suggest a left parietal dominance (Mehta & Newcombe, 1991). Functional neuroimaging studies suggest bilateral activation, greater on the right (Corballis, 1997). Spatial imagery tasks such as mental rotation have been associated with both inferior and superior parietal areas (Alivisatos & Petrides, 1997; Cohen et al., 1996; Kosslyn, DiGirolamo, Thompson, & Alpert, 1998; Parsons et al., 1995; Vanrie, Beatse, Wagemans, Sunaert, & Van Hecke, 2002). The inferior parietal lobule has also said to be involved in coding spatial relationships among objects (Jeannerod & Jacob, 2005). Other evidence suggests that the superior portion of the parietal lobe mediates visually guided action, whereas the inferior portion subserves spatial processing within multiple frames of reference (Colby & Goldberg, 1999); Anderson & Snyder, 1997). Certainly, the variance between these findings suggests a highly complex network of cortical connections that are likely to subserve the component processes involved in visuospatial analysis.

D. The Current Study

Because efficient processing of information depends, to a great extent, on the structural properties of connecting pathways, investigations of white matter integrity can provide information about the neuroanatomic underpinnings of the observed visuospatial deficits evident in children with infantile nephropathic cystinosis. Indeed, the available literature suggests that white matter may be preferentially affected in this group, as cystine crystals have been identified in oligodendrocytes and perivascular macrophages.

Other findings suggest that pre-oligodendroglial cells (i.e., precursors to myelin-forming oligodendroglia) show susceptibility to oxidative stress as can result from the metabolic processes characteristic of cystinosis.

Building from this evidence, DTI was employed as a means of exploring white matter integrity, as it allows for microstructural examination of cerebral tissue beyond that accessible by conventional MR imaging. Given the specific visuospatial impairment found in children with cystinosis, there may also be region specific variation in white matter integrity, as would be reflected in varying anisotropy and diffusivity values. Accordingly, the nature and extent of observed deviations in FA and MD was examined on a whole brain voxel-level and from selected regions of interest, including the parietal (bilateral inferior parietal lobule (IPL) and superior parietal lobule (SPL)) and temporal areas (bilateral inferior temporal gyrus (ITG)) in order to examine whether alterations in the structural constituents of the dorsal stream are evident and whether they occur in the presence of intact ventral stream pathways. Visuospatial performance and cystine levels were examined concurrently to model the relationship between cystine accumulation, white matter pathology, and cognitive function. Investigation of such relationships in a young group is important for determining whether early processes in this genetic disorder adversely affect myelin formation and the development of cortico-cortical projections necessary for complex processing abilities.

The current study tested the following hypotheses:

Hypothesis 1a

The observed visuospatial deficits in children with infantile nephropathic cystinosis are associated with disruptions in white matter integrity in the dorsal visual pathway (the "where" system). These changes will be reflected in attenuated FA in parietal regions of the brain as compared to control children.

Hypothesis 1b

The integrity of the ventral visual pathway (the "what" system) will be comparable between cystinosis and control children. This pattern will be represented by non-significant differences in FA in inferior temporal regions.

Hypothesis 2

Parallel to the anatomical dissociation of the "what" and "where" pathways (Ungerlieder & Mishkin, 1982), there will be a dissociation in FA in the cystinosis group, such that anisotropy values in the temporal regions will be greater than those in parietal regions.

Hypothesis 3

In children with cystinosis, the severity of the visuospatial deficit will be negatively correlated with FA in parietal regions.

Hypothesis 4a

White blood cell cystine level (near the time of testing) will be negatively correlated with visuospatial function and FA in the parietal region.

Hypothesis 4b

Greater variance in cystine levels over one's lifetime will be associated with poorer visuospatial function and attenuated FA in the parietal region.

For the above hypotheses, the inverse relationship is expected for MD.

II. Methods

A. Participants

Forty-eight children ranging in age from three through seven years (mean age, 5.5 ± 1.3 years) participated in the current study. Twenty-four of these children (10 male, 14 female) were diagnosed with infantile nephropathic cystinosis. A control group consisting of 24 typically developing children (12 male, 12 female) were individually matched to the cystinosis children on the basis of age (± 6 months) and socioeconomic status. The diagnosis of cystinosis was confirmed based on genetic testing or elevated leukocyte cystine levels (Smith, Furlong, Greene, & Schneider, 1987; Smolin, Clark, & Schneider, 1987) in addition to clinical history. All cystinosis participants were screened to ensure that they were not experiencing renal failure at the time of testing, that they were euthyroid, had adequate vision for testing, and were free from other neurological conditions. In addition, we ensured that no cystinosis children in our study had a history of pulmonary dysfunction or diabetes mellitus, due to the potential impact of these conditions on neurobehavioral functioning. Cystinosis children were recruited through the National Cystinosis Foundation, the Cystinosis Research Network, and the Cystinosis Research Foundation, all of which maintain close contact with many cystinosis families. Children from many parts of the country were brought to San Diego, accompanied by a parent to participate in the study. Control participants were recruited through newspaper advertisements and from the UCSD subject pool. All potential controls participants were screened with a comprehensive medical history questionnaire and the age-appropriate Wechsler Intelligence Scale to insure that no neuro-developmental, intellectual (IQ < 80), behavioral, or psychiatric problems were present. Additionally, a clinical

neuroradiologist, blind to subject identification, performed a clinical assessment of each neuroimaging study. If pathological findings (e.g., lesion, cystic tissue, volume loss) were evident from neuroradiological review of imaging studies, control participants were excluded accordingly. Two controls and one cystinosis child were excluded due to neurological abnormalities such as an arachnoid cyst or gray matter heterotopia. Demographic characteristics and neuroradiological findings for the cystinosis group are presented in Table 1. Informed consent was obtained prior to testing each participant in accordance with SDSU and UCSD Institutional Review Board procedures.

B. MR acquisition

All participants were imaged without sedation in a 1.5-T GE Signa magnet (EXCITE Version). The diffusion weighted imaging method consisted of a single-shot dual spin echo echo-planar image with b-values of 0 and 2,000 s/mm^2 (TR = 105ms, TE = 82.2ms, FOV = 24cm, Flip angle = 90°, fractional k-space acquisition 128 x 128 interpolated to 256 x 256, 3.8mm contiguous slices). The diffusion sampling scheme is the simple model method of Basser and Pierpaoli (1996), which assumes Gaussian diffusion and can be described by a symmetric 3x3 diffusion tensor (**D**) and hence, requires 6 different diffusion weighting directions and a seventh normalizing image with b = 0 (gradient coordinate system (*x*,*y*,*z*): (0,1,1); (0,1,-1); (1,0,1); (1,0,-1); (1,1,0); and (1,-1,0). Two series were collected to correct for motion and were externally averaged.

High resolution structural T1-weighted axial images were acquired using a spoiled gradient echo (SPGR) sequence (TR = 400ms, TE = 14ms, FOV = 24cm, Flip angle = 90°, Matrix = 128 x 128 interpolated to 256 x 256, 3.8mm contiguous slices)

covering the entire cerebral volume to provide an anatomical reference and allow for spatial registration of the diffusion images, as required for voxel-based analysis. High resolution T1-weighted sagittal images also acquired using a using a spoiled gradient echo (SPGR) sequence (TR = 20ms, TE = 4ms, FOV = 25cm, Flip angle = 90°, Matrix = 128 x 128 interpolated to 256 x 256, 1.3mm contiguous slices) covering the entire cerebral volume, provided an anatomical reference for manual definition of regions of interest.

C. Pre-processing

Diffusion and SPGR images were transferred to a separate workstation (Silicon Graphics 2000, Calif., USA) for post-processing. Data were visually inspected for sufficient quality. Although the dual spin echo echo-planar sequence greatly reduces eddy current distortions caused by the diffusion weighted gradients, a qualitative examination was conducted to ensure that this technique worked sufficiently. Those data deemed invalid due to technical problems or artifacts (e.g., eddy current, susceptibility, ghosting, motion) were excluded from the study. Four participants (2 cystinosis, 2 controls) were excluded due to severe motion artifact. Two participants (1 cystinosis, 1 control) were excluded due to susceptibility artifacts.

Following data inspection, each diffusion-weighted brain volume was aligned using a transformation algorithm (translations only) to correct for motion occurring between the two images sets at acquisition using the commercial software package Amira 3.1 (http://amiravis.com; Mercury Computer Systems Inc., Chelmsford, MS, USA). Within each image set, alignment was performed between each diffusion weighting

direction and between the diffusion images and the normalizing ($b = 0$ s/mm^2) images. Once completed, the two image sets were averaged to improve signal-to-noise ratio.

To ensure inter-individual anatomical alignment, the T1-weighted axial and sagittal images of all subjects were AC-PC aligned in SPM2 (Statistical Parametric Mapping, Welcome Department of Imaging Neuroscience, University College London). The FA and MD maps (see details on calculation below) were then coregistered to the SPGR images using a mutual information method. Segmentation of the T1-weighted axial and sagittal images into three separate tissue classes representing gray matter (GM), white matter (WM), and cerebrospinal fluid (CSF) was completed using an automated algorithm in SPM2. This method employs a combined a priori knowledge and pixel intensity approach, resulting in tissue probability maps (Ashburner & Friston, 1997) The segmented white matter images were used as masks from which to extract FA and MD values (Schmithorst 2002, Barnea-Goraly, 2005).

D. DTI Quantification

Using Analysis of Functional NeuroImages' (AFNI; http://www.afni.nimh.nih.gov; Cox, 1996) diffusion plugin routine (3dDWItoDT), the components of the diffusion tensor were computed. Based on the methods proposed by Basser and Pierpaoli (1996), the diffusion tensor is calculated from the 6 independent diffusion directions acquired for each subject using a multivariate linear regression. From the diffusion tensor, the overall displacement of the molecules (average ellipsoid size) is characterized by calculating the mean diffusivity (MD). To do so the trace (Tr) of the diffusion tensor, which is calculated as the sum of the eigenvalues of the tensor is used to

compute the MD. The diffusion tensor is then diagonalized to yield eigenvalues (λ_1, λ_2, λ_3) as well as eigenvectors that define the predominant diffusion orientations. On the basis of the eigenvalues from the tensor, fractional anisotropy (FA) is calculated. Values of MD and FA are calculated on a voxel-by-voxel basis to create separate images, or maps, of each index. The FA and MD maps are computed in the original native coordinates of the acquired images before any registration operations are applied to the scalar values.

The following equations are applied:

$$ADC = \frac{1}{3}Tr(\mathbf{D}) = \lambda_1 + \lambda_2 + \lambda_3 = D_{xx} + D_{yy} + D_{zz}$$

where Tr(**D**) is the trace of the diffusion tensor, an index that is invariant to the orientation of the reference frame. The MD is measured in $x10^{-6}$ mm^2/s.

$$FA(\mathbf{D}) = \sqrt{\frac{1}{2}}\frac{\sqrt{(\lambda_1 - \lambda_2)^2 + (\lambda_2 - \lambda_3)^2 + (\lambda_3 - \lambda_1)^2}}{\sqrt{\lambda_1^2 + \lambda_2^2 + \lambda_3^2}}$$

FA is a unitless index where a value of 0 represents an isotropic medium with no directionality to diffusion and a value of 1 represents maximum anisotropy.

E. Voxel-Level DTI Analysis

Due to the paucity of literature characterizing the neural substrates of cystinosis, a voxel-based analysis was performed as an initial step. Following coregistration of high-resolution anatomical (T1-weigthed axial) images and diffusion maps, the images were transformed into a standardized space. Given that the use of adult reference data in a pediatric study introduces severe bias into tissue classification and normalization procedures, a pediatric brain template was utilized for normalization of images (*CCHMC pediatric brain template*, 2001; Wilke, Schmithorst, & Holland, 2003). The pediatric template (*CCHMC2_young*) consists of 67 children ranging from 5 to 9.5 years of age. Images were transformed using a linear affine transformation with 12 degrees of freedom and nonlinear deformation (Friston et al., 1995). Normalization parameters were calculated from the high-resolution T_1-whole brain image. The resultant spatial transformation parameters were then applied to the quantified FA and MD. The spatial normalization procedure reformats the images to 91 slices with 1 x 1 x 4 mm^3 resolution.

The FA and MD maps were smoothed with Gaussian kernels with full width half maximum (FWHM) of 8 mm, 10 mm, and 12 mm, due to a recent study indicating that incremental smoothing kernels can lead to different conclusions (Jones, Symms, Cercignani, & Howard, 2005). In our study, the size of the clusters SPM identified increased with smoothing, though no clusters "appeared" or "disappeared" when different kernels were applied. The 8 mm smoothing kernel was applied and retained for statistical analysis, as this allows anisotropy data to better conform to a Gaussian field model by reducing the proportion of voxels exhibiting nonnormally distributed residuals (Jones et al., 2005). This kernel appeared desirable over larger ones that are frequently used in

SPM analysis of DTI given the heterogenous nature of FA maps as well as the need to preserve reasonable image resolution.

Statistical analysis was performed using an independent samples t-test paradigm to compare the cystinosis and control groups. A statistical threshold of $p<0.001$ was initially applied (height threshold) and set at 5 voxels. An extent threshold of $p< .05$ corrected for multiple comparisons was applied at the group level. Two contrasts were used to detect whether each voxel had a higher or lower mean diffusivity or fractional anisotropy in the cystinosis group compared with the control group. Increases or decreases were deemed to be significant at the cluster level (=> 5 voxels) when the p-value was less that 0.05 after correcting for multiple comparisons. The anatomic location of each cluster was determined with the help of neuroanatomy atlases (Jelacic, de Regt, Weinberger, 2006; Mulligan, K.A., & Sundsten, Ph.D. (1998).

F. ROI-Based DTI Analysis

As a second step, mean values for the different diffusion parameters (FA and MD) were calculated from specified regions of interest. Based on previous findings of the probable anatomical correlates of visuospatial function, selected regions of interest including the left and right IPL (LIPL; RIPL), the left and right SPL (LSPL; RSPL), and for purposes of demonstrating a dissociation, the left and right ITG (LITG; RITG) were defined. The purpose of this procedure was to illustrate the magnitude of effects demonstrated by the voxel-based analysis, and extend findings by reducing Type II error rate secondary to conservative statistical thresholding required in voxel-based analysis. The ROI method also allows us to measure the association of clinical variables with the

independent variables (FA and MD) in regions that are specified a priori and require no morphing for definition. In addition, anatomical ROIs localize the differences in individuals' brains more accurately than whole-brain normalization into a standard space (Nieto-Castanon et al., 2003).

The ROIs were defined in Amira by manually tracing the regions onto the high resolution T1-weighted sagittal images. The resolution of these images allowed for greater precision during ROI definition. Manual definition was implemented to minimize the confound of including adjacent structures (Schneider et al., 2004; Snook et al., 2005). Such outlining confers an advantage over faster but more simplistic methods of placing geometric shapes over a certain area or interpolating over the brain volume. Each region's limiting sulci, gyri and other anatomical landmarks were located by viewing the structural images in three orthogonal planes. Use of a surface rendering algorithm (Amira Voltex) allowed for a three-dimensional (3D) view of the relevant structures. The 3D images could be rotated around x, y, and z axes, to achieve the best possible visualization of each ROI. The outlines of the ROI are drawn around relevant brain regions and the Amira routine then fill in the region, thus defining the interior of the outline as the ROI.

Standardized rules were applied for delineating each region, applying definitions provided by previous research protocols (Laboratory of NeuroImaging, UCLA). The parietal lobe was traced first (Figure 2a) before parcellation into superior and inferior lobules. The parietal lobe is bounded by the frontal lobe, occipital lobe, and cingulate gyrus. The fronto-parietal border was defined by the central sulcus and the parieto-occipital fissure marked the posterior border. The parietal lobe was traced primarily in the sagittal plane, beginning off center from the midline. Tracing progressed laterally in

the sagittal plane. As the corpus callosum disappears, the lobe was traced as all matter above the lateral ventricle extending to the tip of the hippocampus. Following definition of the parietal lobe, the postcentral gyrus was extracted and the remaining region was subdivided in to IPL and SPL. The anatomical boundaries of the IPL consisted of the post-central sulcus as the anterior border, the intraparietal sulcus as the superior border, and the lateral fissure as the anterior inferior border. The SPL emerges medial to the supramarginal and angular gyrus and is bounded anteriorly by the post-central sulcus and posteriorly by the parieto-occipital fissure. The ITG was located and drawn on both the lateral and ventral surfaces of the hemisphere using boundaries including the inferior temporal sulcus and occipito-temporal sulcus (Kim et al., 1999). Tracing of the ITG terminated medially as the insula fused with the superior temporal gyrus. Each region was defined in both hemispheres.

The interrater reliability of the ROI-defining procedures was obtained for each region between two trained staff members. Reliability for each ROI was evaluated in three randomly selected cases assessed by the two raters, who performed tracing blind to diagnosis. Intraclass correlation coefficients were 0.95 for the LSPL, 0.96 for the RSPL, 0.95 for the LIPL, 0.97 for the RIPL, 0.96 for the LITG, and 0.96 for the RITG.

Following ROI definition, ROI masks were applied to FA and MD maps in order to calculate statistics from the defined region. Segmented white matter images were first multiplied by the ROI mask to exclude gray matter and CSF from the ROI. The resulting white matter ROI mask was applied to FA and MD maps, were mean values were extracted (Figure 2a-d depicts this process). Mean FA and MD values were imported into SPSS 15.0 (SPSS, Inc., Chicago, Illinois, USA) for statistical analysis.

G. Visuospatial Assessment

Two measures of visuospatial cognition were administered to each participant to examine whether changes in FA and MD were associated with behavioral performance. The Spatial Relations test of the Woodcock-Johnson Psycho-Educational Battery was used to assess visuospatial abilities (McGrew & Woodcock, 1985). This test was selected as it has shown sensitivity to the visuospatial deficits in the cystinosis group (unpublished data). In the Spatial Relations test the participant is required to visually select from a series of shapes the component parts required to make a whole. Shapes become increasingly more abstract and complex as the test progresses. Mental rotation of component parts is required to form a correct whole. A three minute time limit applies. Normative data are provided for ages 3 to 80+ years. A raw score based on number of correct responses is converted to a standard score, standardized for age. Standard scores have a mean of 100 (SD = 15).

The Beery-Buktenica Developmental Test of Visual Motor Integration, 5th Edition (VMI) (Beery and Beery, 2004) assesses the integration of visual and motor abilities. Scarvie, Ballantyne, and Trauner (1996) demonstrated sensitivity of this measure to visuospatial impairments in children with cystinosis. The Copy and Coordination component of this measure consists of 27 geometric forms presented in developmental sequence. Participants are asked to copy each form in successive order. All protocols are scored by two independent raters to ensure interrater reliability equivalent to at least 95% overall agreement. Scores are then standardized for age.

Standard scores have a mean of 100 (SD 15). Normative data are provided for children ages 2 through 18 years.

In addition to the measures above, all participants were administered either the Wechsler Preschool and Primary Scale of Intelligence-Revised (WPPSI-R) (Wechsler, 1989) or the Wechsler Intelligence Scale for Children-III (WISC-III) (Wechsler, 1991), depending on age.

H. Cystine Levels

Cystinosis participants' past and current white blood cell cystine levels were obtained from medical records. The appropriate HIPAA research authorization was obtained from parents prior to accessing cystine lab panels. Cystine levels were analyzed in traditional units (nmol of half-cystine per milligram of protein). Analysis of cystine level with diffusion maps and visuospatial functioning was performed if cystine measurements occurred within two months of participation in the study. Lifetime cystine levels were analyzed if two measurements at minimum were collected over each year of life.

I. Statistical Analysis

Prior to analysis, independent and dependent variables were examined through SPSS for accuracy of data entry, missing values, and fit between their distributions and the assumptions of multivariate analysis. Variables were examined separately for the 24 cystinosis participants and 24 control participants. Initial data screen indicated no missing values in the dataset. Frequency and descriptive statistics indicated an even split

for gender (45.8% male and 54.2% females). Distributions of continuous variables were also examined. While cognitive measures had a normal distribution, others variables including FA, MD and cystine level were nonnormally distributed. Accordingly, planned comparisons were performed in a parametric framework in order to model covariates (detailed below). However, analyses were replicated using nonparametric methods where appropriate, so as to ensure the accuracy of our findings.

A multivariate analysis of variance (MANOVA) was used to test for group differences in FA and MD (Hypothesis 1a&b), as this model does not assume spherecity. As brain structure and diffusion properties change with age and differ between boys and girls (Schmithorst, Holland, & Dardzinski, 2007)**,** we tested the effect of potential covariates including age and sex on FA and MD in cystinosis patients and controls.

Hypothesis 2 was also tested using a multivariate framework (MANOVA) to examine the relationship between parietal and temporal FA and MD. Spearman correlations were performed to assay the relationship between visuospatial performance and FA/MD in parietal regions (Hypothesis 3). Similarly, Spearman correlations were employed to examine the relationship between cystine level, visuospatial function and FA/MD in parietal regions (Hypothesis 4a&b).

III. Results

Examination of our data distribution revealed one outlier in the cystinosis group with extremely low (FA) z-scores in the parietal regions. However, influence statistics including Cook's distance (critical value = 13.79, maximum sample value = 9.31) as well as DFFIT, DFBETA, and DFBETAX, did not identify this case or any others as multivariate outliers in their respective groups. Moreover, analyses were repeated while omitting this participant and findings remained unchanged.

A. Behavioral Performance

A multivariate analysis of covariance was performed on two measures of visuospatial functioning and two measures of intellectual functioning (WJ-III Spatial Relations Subtest, Beery VMI, Wechsler VIQ, and Wechsler PIQ) to compare performance between the cystinosis and control groups, with age as a covariate. There was a significant main effect of group ($F(1,46) = 36.87$, $p<.0001$), such that the cystinosis group performed worse than controls overall. Using Wilks' lambda, there was also a main effect of measure ($F(3,44) = 10.35$, $p<.0001$). Simple effects analysis revealed that participants in both groups performed worse on the VMI as compared to Spatial Relations ($p<.0001$). Comparison of overall profiles did not indicate significant deviations from parallelism. See Table 2 for descriptive statistics.

B. Voxel-Level DTI Analysis

We evaluated the relationship of demographic variables such as age and gender with FA/MD as a preliminary step. Spearman correlations indicated a positive

relationship between age and FA in the cystinosis group in the following white matter regions: (1) right mid-occipital gyrus, (2) right mid-temporal, (3) right frontal sub-gyral, (4) left limbic lobe, (5) right inferior parietal lobe (False Discovery Rate (FDR)-corrected, $p<.001$). No significant relationship between age and FA was found in the control group. Analyses evaluating the relationship between age and MD did not reveal any significant relationships for either the cystinosis or control group. No difference in FA or MD was apparent between males and females. Given the interaction between age and group, age was included as an independent variable in further analyses.

Whole brain voxel-level analysis revealed a number of spatially distinct brain regions with decreased FA in children with cystinosis relative to controls. The white matter regions included the following: (1) bilateral superior parietal, (2) bilateral sublobar inferior to region 1, (3) right inferior parietal, (4) right mid-temporal gyrus (5) right medial and superior frontal gyrus and (6) right cingulate gyrus (FDR-corrected, $p = .031$) (See Figures 3-5). No regions were identified in the cystinosis children where FA exceeded that of controls. No significant differences in MD were evident between groups. Nonparametric analyses replicated the above findings.

C. ROI Analysis

To expand the voxel-based analysis on a single subject level, a region of interest (ROI) analysis was conducted focusing on brain regions of greatest theoretical relevance to visuospatial cognition (bilateral parietal lobes). For the purposes of demonstrating a dissociation, structures implicated in perceptual cognition (bilateral inferior temporal

regions) were also defined. The selected parietal ROIs corresponded to results of thresholded statistical maps obtained in the voxel-level analysis.

As performed in the voxel-level analysis, potential covariates including age and gender in relation to FA and MD were evaluated. The following analyses employed Hochberg correction for multiple comparisons, maintaining $\alpha_{FW} = .05$. Analysis of FA and MD constituted separate families of comparisons. Spearman correlations indicated a positive relationship between age and FA in the LIPL (r=.45, p=.03), LSPL (r=.46, p=.02), RIPL (r=.43, p=.03), and RSPL (r=.56, p=.005) for the cystinosis group only. These data are presented in Figure 6a-d. Significant negative correlations between age and MD were evident in the LIPL (r=-.49, p=.01), RIPL (r=-.61, p=.001), and RSPL (r=-.46, p=.02) in the cystinosis group and in the LIPL (r=-.41, p=.04) for controls. No differences in FA or MD were apparent between males and females. As with voxel-level analysis, age was included as an independent variable in further ROI analyses.

In controls, FA and MD values were symmetrical across parietal regions. In cystinosis patients, one area of asymmetry was evident. Fractional anisotropy was significantly lower in the RIPL as compared to the homologous region in the left hemisphere (T(23) = 2.60, p=.02). A between-group comparison using MANOVA revealed significantly decreased FA in cystinosis participants as compared to controls in the bilateral SPL and RIPL as seen in Table 3. No group differences in FA were evident in temporal regions. Using the same analytic model, we found increased MD in the cystinosis group bilateral SPL as compared to the controls (Table 4). No between-group differences in MD were evident in temporal regions. Nonparametric statistics using the Mann-Whitney U Test replicated the findings above, though significantly increased MD

in the cystinosis group was additionally evident in the LIPL (z=-2.17, p=.03) and RIPL (z=-2.0, p=.05).

Interestingly, alterations in FA were more pronounced for younger cystinosis children, whereas older children with cystinosis had mean FA values that approximated that of controls. This pattern of development, illustrated in Figure 6, suggests a possible lag in neuromaturation.

Contrary to expectations parietal regions had significantly higher FA values than temporal regions in the left ($F(1,45) = 76.78$, $p<.0001$) and right hemisphere ($F(1,45) = 135.76$, $p<.0001$) in both groups. Parietal regions also had significantly lower MD values than temporal regions in the right hemisphere ($F(1,45) = 4.94$, $p=.031$). A significant group x region interaction emerged in the comparison of MD values in the left hemisphere. Controls demonstrated significantly lower MD values in left parietal regions as compared to left temporal regions ($T(23) = -3.63$, $p = .001$), whereas children with cystinosis did not demonstrate lower MD values in left hemisphere parietal regions. Nonparametric statistics using the Wilcoxon-Signed Ranks Tests were consistent with the above findings.

Additional analyses were performed for subgroups of cystinosis participants with normal radiological brain MRI scans to address the potential confound of white matter pathology as contributing to differences between groups. In addition, a similar analysis was performed excluding those children with gray matter pathology. These analyses generally replicated those already described. In particular, even after selecting cystinosis participants without evidence of overt brain pathology, patients continued to show reduced FA in parietal regions as compared to age-matched controls.

D. Correlation with Clinical Data

No significant relationship emerged between FA or MD in parietal regions and visuospatial functioning for either group. Given the significant relationship between age and FA/MD found only in the cystinosis group, additional analyses were conducted on a subset of cystinosis participants to examine whether age moderated correlations between FA/MD values and visuospatial functioning. Analysis of school-aged cystinosis participants (age > 5.50, n = 13) revealed a positive relationship between FA in the RIPL and performance on the Beery VMI (r= .74; p=.004). Results of analyses repeated to evaluate temporal regions, revealed no significant relationship between FA/MD and visuospatial functioning.

Examination of the relationship between cystine levels and FA/MD (n = 17) revealed a positive relationship between white blood cell cystine level at the time of testing and RSPL MD (r = .50, p=.04) and a similar trend in relation to the RIPL MD (r=.46, p = .05). Analysis of the school-aged cystinosis participants (age > 5.50, n = 10), extended findings from the total group. Specifically, positive relationships between cystine level at the time of testing and LIPL MD (r = .93, p=.001), LSPL MD (r = .91, p=.002), and RIPL MD (r = .86, p=.007) were evident. A trend toward a negative relationship between cystine level and RSPL FA was also noted (r = -.69, p=.06). Additionally, greater variance of cystine levels over one's lifetime was associated with decreased PIQ (r=-.72, p=.04). Results of analyses repeated to evaluate such relationships in temporal regions, revealed no significant findings.

IV. Discussion

The current study investigated white matter microstructure, as measured by DTI, in young children with cystinosis. In light of the visuospatial impairments documented in this group, the specific objective of this study was to address the hypothesis that white matter integrity in areas constituting the dorsal visual pathway would be compromised in children with cystinosis. It was also hypothesized that this finding would occur in the context of intact ventral visual pathways, consistent with the anatomical and behavioral dissociation of the two visual streams. A second objective was to characterize the relationship between diffusion parameters in the dorsal regions and visuospatial performance. Given the increased efficiency and refinement of cognitive skills with white mature maturation, diffusion anisotropy was expected to positively correlate with visuospatial performance. Beyond this proposed brain-behavior relationship, we predicted that cystine accumulation, as signaled by the genetic deletion in cystinosis, would reveal additional important information at the neurobiological level. Given that cystine accumulation and resultant crystal formation can adversely affect parenchymal microstructure, we hypothesized that elevated white blood cell cystine levels would be associated with evidence of deficient white matter integrity. Together, the objectives of this study provided a framework from which we could begin to understand the pathogenesis of neurocognitive deficits in this rare condition.

A. Overall trends from voxel-level analysis

Given the paucity of literature characterizing the neural substrates of cystinosis, a whole-brain voxel-level analysis was conducted to describe overall differences between

children with cystinosis and their typically developing peers. Findings revealed lower mean FA in children with cystinosis as compared to controls in parietal regions including the bilateral SPL and right IPL. Other areas bearing similar attenuations occurred in the bilateral fronto-parietal sublobar regions, and in a number of right hemisphere structures including the mid-temporal gyrus, medial and superior frontal gyrus and cingulate gyrus. These findings parallel results of a recent voxel-based morphometry study investigating cerebral grey matter volume in this group. Findings indicated focal grey matter decreases in the left inferior parietal region, as well as the right superior parietal lobule (Sach et al., 2007).

The spatially distinct regions identified in our voxel-wise DTI analysis have been collectively identified in the literature as being critical to visuospatial processing. In a functional magnetic resonance imaging (fMRI) study of spatial working memory in children (9-18 years of age), activation in the bilateral inferior and intraparietal cortex, bilateral middle and superior frontal gyrus, and right cingulate gyrus positively correlated with performance (Nelson et al., 2000). These fronto-parietal networks appear to support complex spatial processing including visuospatial working memory. Consistent with this model, an adult study focusing on dorsal stream activation during a binary decision-making task found primary bilateral parietal activity in addition to mid-temporal, frontal, and cingulate activation while making judgments with respect to the shape and size of common objects (Oliver et al., 2003). Similar patterns are reported in clinical child populations with visuospatial deficits such as Williams syndrome (Atkinson et al., 2003) and fragile X syndrome (Kwon et al., 2001), where nonverbal processing deficits predominate.

B. Changes in dorsal stream diffusion anisotropy

To extend findings from voxel-level comparisons, a region of interest approach was employed to examine more focused comparisons of FA and MD within the parietal and temporal brain regions. Consistent with our hypothesis, children with cystinosis evidenced diminutions in mean FA in component areas of the dorsal visual pathway. Specifically, these areas included the bilateral SPL and right IPL. A concomitant increase in MD was evident not only in these regions, but also in the left IPL. In children with cystinosis, we found no alterations in FA or MD in the bilateral ITG, a predominant region constituting the ventral visual pathway. Bilateral decrements in FA in children with cystinosis appear consistent with the bilateral profile that young children demonstrate when performing visuospatial tasks (Jones et al., 2000). Together, these findings suggest that selective changes in cerebral white matter are evident in cystinosis and are present early on in development. In tandem with voxel-level analysis, our results further suggest that there may be disruption in more distributed areas including fronto-parietal networks and mid-temporal pathways important for spatial working memory.

Contrary to expectations, children with cystinosis did not demonstrate decreased FA values in dorsal relative to ventral regions. In fact, the reverse pattern was observed. This finding was also evident in controls. Given that the variances associated with mean FA estimates were similar across parietal and temporal regions, it does not appear that differences in regional volume or region selection can explain these findings. It is possible that inherent histological differences in inferior temporal white matter structure such as reduced coherence of fiber pathways result in relatively lower FA values as compared to parietal regions. At present, there is no such description in the literature

from which to compare our values. Aside from structural differences, it must also be considered that our DTI collection utilized an EPI MRI sequence, which suffers from signal dropout due to field inhomogeneity induced by the differential susceptibility of brain tissues (Liu et al., 2003). These artifacts are most severe at air-tissue interfaces near the temporal lobes and at surroundings of sinuses. This likely results in a less robust estimate of FA and MD in the above mentioned vulnerable areas and may contribute to the 'low FA values' noted in the ITG in both groups. Applying techniques that minimize such distortions such as using segmented instead of single-shot EPI or using STEAM sequences which are insensitive to susceptibility artifacts and eddy currents (Notle et al., 2000) would be beneficial for comparison and validation of values in this region.

C. Diffusion anisotropy changes with age

Beyond understanding the nature of CNS pathology in cystinosis, the evolution of neuropathology has remained a central question in characterizing this condition. Specifically, does the genetic deletion in cystinosis cause early structural alterations or do progressive disease processes result in compromise of structure over time? Though this is best investigated with a longitudinal design, the present findings provide some insight regarding neurodevelopmental processes in this disorder. Our study demonstrated significant positive correlations between age and diffusion parameters in children with cystinosis, whereas control children generally exhibited a relatively flat profile across the age range studied. The latter finding is in agreement with studies describing MD and FA over the developmental period. Specifically, diffusion parameters measured in multiple cerebral regions including the frontal white matter, caudate, thalamus, corpus callosum,

internal capsule, and periventricular white matter show a rapid increase in FA and decrease in MD during the first 2 years of life. Following this steep pattern, is a slower process of change on through adolescence (Zhang et al., 200 Mukhergee, 2001; 2002). The slope of FA from 2 to 18 years of age is modest in magnitude particularly for regions subserving higher cognitive functions, in which development is relatively more protracted.

A study investigating diffusivity and anisotropy over the period from 5 – 18 years of age, showed areas of significant positive correlation with FA predominantly in motor projection fibers such as the internal capsule and corticospinal tract. Highly compact tracts including the inferior longitudinal fasciculus and arcuate fasciculus also showed correlations with FA. By comparison, changes in frontal and parietal areas were not significantly apparent (Schmithorst et al., 2002). Illustrating this point further, a comparison mean FA derived from two groups, one 12 to 35 months of age, and a second 36 to 71 months of age, indicated a mean increase in FA of only 7% in fronto-parietal white matter between the younger and older groups.

Children with cystinosis show a departure from this developmental pattern. Examination of age-related changes in FA in cystinosis children revealed a notable developmental lag at young ages in comparison to control children. Young children with cystinosis demonstrated significantly lower mean FA in bilateral parietal regions relative to their peers. While they appear to catch-up by the age of 5.5 years, as reflected in comparable mean FA values to control children, they continue to demonstrate cognitive deficits. This finding is particularly striking as it suggests that the structure of the fiber networks may be inefficiently laid down early in development. Aberrations in the core

framework may result in persistent cognitive deficits that cannot be overcome with maturation. Moreover, initial changes in myelin precursors or cellular components may result in altered white matter maturation.

D. Clinical correlates of mean diffusivity and diffusion anisotropy

Correlation of diffusion parameters with visuospatial performance indicated a significant positive correlation between FA in the RIPL and performance on a task of visual motor integration. However, this relationship was evident only in school-aged children with cystinosis (>5.5 years). Given that brain regions involved in spatial analytic processing become more specialized over the course of development, particularly from 6 –12 years of age (Aksoomoff & Stiles; 1995), the relationship between FA and performance on visuospatial tasks may not be entirely discernable in younger children with cystinosis (< 5 years). Although mean FA in school-age children with cystinosis may begin to approximate that of controls, the nature of fiber organization and connectivity may be qualitatively different, and thus lead to disparate visuospatial cognitive abilities. As the visuospatial performance of cystinosis children reported here did not demonstrate the typical profile of uniformly impaired spatial processing in the context of preserved perceptual and verbal intellectual functioning (Trauner et al., 2007), relationships between FA and visuospatial performance may be less pronounced in our sample than is true for this age group of cystinosis children.

A tertiary component of our study focused on a neurobiological marker in cystinosis, namely cystine, to explore potential mechanisms of white matter pathogenesis. High white blood cell cystine levels reflect increased cystine accumulation, which

interferes with cellular structure and function (Feksa, 2004; Gahl, 1986). Cystine is therefore a critical variable in pathology, as underscored by our findings. Regardless of age, white blood cell cystine level was found to positively correlate with MD in the right SPL with a similar trend evident in the IPL. While cystine accumulation and resultant crystal formation would be expected to hinder diffusion, it appears that either a breakdown of existing white matter pathways or a stunting of white matter development may be a consequence instead. The latter possibility fits well with the developmental lag in FA described earlier.

Older cystinosis children (> 5 years) not only demonstrated stronger associations between cystine level and MD, but the relationships were evident in bilateral parietal regions. This suggests that in addition to an initial disruption in white matter maturation early in development, there may be a secondary progressive effect of cystine accumulation on white matter organization and connectivity. Of note, we begin to see the effect of increased cystine on FA in the older cystinosis group, where we observed a trend toward a negative relationship between cystine level and FA in the RIPL. Although only speculative, this trend may presage regressive processes in the adolescent period. Indeed, in their study of visuomotor integration in children with cystinosis (4 – 16 years of age), Scarvie, Ballantyne, & Trauner (1996) showed that with advancing age, children with cystinosis fell further behind their typically developing peers. This could reflect early underlying structural alterations that give rise to 'hypofunctional' cortical networks, possibly a cumulative effect of cystine over time, or a combination of both processes.

Although cystine level was not systematically related to visuospatial performance, increased variation in cystine levels over time corresponded to decrements in PIQ (in

children > 5 years of age). As alluded to above, established structural networks which may be inefficiently laid down may also be increasingly vulnerable to fluctuations in disease load. The current study suggests that variation in cystine over the course of development is an important factor in the pathogenesis model of cystinosis.

E. Diffusion parameters and implications for neuropathogenesis

The pathogenesis of neuroanatomical alterations in cystinosis is presently unknown, though the current study provides a basis for speculation in this regard. Alterations in both FA and MD in children with cystinosis may be reflective of a number of abberant neurodevelopmental processes. Increased amounts of intraaxonal fluid may be caused by inadequate microtubule or microfilament production, leading to increased diffusivity and decreased anisotropy. Concomitant increases in extracellular water volume may be due to hypomyelination, poor glial processing, or decreased synaptic density, leading to the same outcome. In addition, immature or abnormal axonal growth can lead to diminished axonal diameter and result in decreased anisotropy.

It is possible that these alterations are present early in development, emerging from aberrations in cellular components and membranous organelles that are directly related to the CTNS gene (Kleta et al., 2004). It is also possible that the accumulation of cystine in the oligodendroglial lysosomes could result in lysosomal degeneration and cell death (Gieselmann, Polten, Kreysing, & von Figura, 1994; van der Knaap, Breiter, Naidu, Hart, & Valk, 1999). In this way, intracellular crystal formation may simulate cytotoxic edema, as occurs in glial cells, axons, and myelin sheaths. An additional consideration is that an interaction of these processes is at work. Initial cellular and membrane damage

set in place at an early point in development may instigate a cascade of events eventually resulting in loss of fiber integrity. This microstructural compromise may be more significantly apparent in adolescence when a number of neuromaturational processes coalesce. Moreover, the relationship between white matter integrity and cognitive functioning may also be more pronounced during this period when complex processing skills are developed and refined.

F. Limitations

Several limitations to the current study must be addressed in future research. Though our population is quite rare, our sample size did preclude more extensive analysis of relationships between demographic, neurobiological, and cognitive variables in this study. It is possible that more widespread differences between children with cystinosis and controls were not obtained due to the limited power of our small sample size. The power was further reduced due to corrections for multiple testing, which could be improved with large sample sizes.

Our methods were also limited with regard to our diffusion protocol and processing techniques. In particular, we utilized a simple 6 direction diffusion model primarily to minimize scan time for our young participants. This model is inappropriate for voxels containing multiple-fiber orientations and can lead to significant error in estimating diffusion parameters (Frank, 2001; Pierpaoli 1996). High angular resolution techniques should be considered in future work to more accurately characterize local diffusion characteristics. As described earlier, an EPI sequence was employed to obtain our diffusion-weighted images, the disadvantages of which included signal loss and

geometric distortions caused by susceptibility gradients. A more quantitative approach to addressing these distortions, such as field map correction, would significantly improve the diffusion parameter estimates in the current study.

Aspects of our image processing technique were also limited. While we used an affine and non-linear normalization procedure (Crivello et al., 2002; Robbins et al, 2004) in the voxel-level analyses to better correct for local differences in our study population, spatial inaccuracies in the coregistration and normalization procedures could confound voxel-level DTI analysis. Although we made efforts to reduce this risk as much as possible, by using a pediatric template based on images from children ages 5-9, this developmental range does not precisely overlap with our group of children (3-7). Also, in our study, the voxels were anisotropic (1 x 1 x 4 mm^3), which renders the data more susceptible to partial volume effects than data with isotropic voxels. Although these dimensions were chosen on a pragmatic basis, to provide an acceptable scan time for young children, this may at least theoretically affect the final results.

Another issue that requires consideration in the current study as well as future studies is the limited cognitive data available. Extending cognitive measurements to assess different aspects of visuospatial functioning may better characterize the nature of the impairments in children with cystinosis as they relate to white matter pathology.

Finally, although our study addresses important hypotheses for understanding the neuropathophysiology of cystinosis, the relationship between DTI measures and specific changes to the white matter structure are still unclear. Changes in FA may be caused by any combination of factors related to myelination, axonal diameter, fiber density, and

coherence. Histological studies may be necessary to identify the specific microstructural white matter changes in cystinosis.

G. Future Directions and Conclusion

One component of visuospatial processing not examined here is that of spatial working memory. Cystinosis children have shown deficits in their ability to process and retain information about location. Given that systematic changes in memory for spatial location have been observed throughout the preschool period (Huttenlocher, Newcombe, & Sandberg, 1994) and well into the school years (Newcomber & Huttenlocher, 2000), this area of cognitive skill may reveal additional information regarding the neurobehavioral profile of children with cystinosis.

Developmental of brain systems that mediate visuospatial function undergo critical change, particularly in early adolescence, when patterns of functional activation begin to resemble that of adults. Examination of this period of development in adolescent children with cystinosis may provide insight into the progression of white matter compromise and related cognitive changes. Longitudinal examination of children in the current study would also elucidate the extent to which early changes in brain parenchyma and progressive processes interact to produce the behavioral phenotype thus far described in cystinosis.

Extending our current analysis to explore fronto-parietal connectivity is also of interest for future study. The prefrontal cortex has been implicated in executive functions underlying visuospatial processing and spatial working memory (Smith and Jonides, 1999). Hence, white matter abnormalities in the right frontal areas in children with

cystinosis may be associated with deficits in executive skill. Indeed, recent work has identified executive difficulties in the nonverbal domain in children with cystinosis (Spilkin et al., 2007), suggesting that this may be an additional area of cognitive vulnerability.

Related to the issue of connectivity, a more detailed description of fiber coherence and organization is prerequisite for understanding the precise nature of white matter compromise in children with cystinosis. Advanced methods such as fiber-tract mapping in combination with functional imaging techniques are ideal for approaching this level of specification.

In conclusion, this study provides new evidence that the average DTI properties in children with cystinosis deviate from typically developing children. These differences are predominant in the parietal regions, but are also present in frontal and mid-temporal areas important for working memory and executive skills. The differences in diffusion anisotropy appear to vary over the early developmental period, where a developmental lag in white matter maturation is implicated. Our findings further suggest that early microstructural changes may impact the development of efficient fiber networks and result in cognitive skill deficits. In addition, ongoing neurobiological processes in cystinosis may constitute a secondary factor impacting overall behavioral outcome.

Our findings are also of clinical significance as they demonstrate early alterations in white matter maturation that may result in subtle, but persistent cognitive deficits. Given the substantial evidence that experience plays a critical role in directing the course of cognitive development, early intervention in the form of visuospatial skill training may result in greater adjustment to initial disruptions in this system.

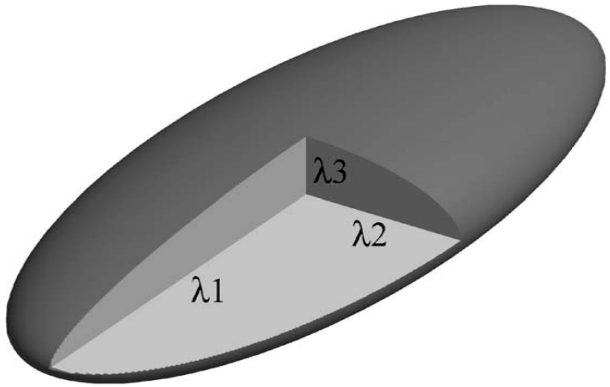

Figure 1. The diffusion tensor displayed as an ellipsoid. The three mutually perpendicular eigenvectors define the principal axes of this ellipsoid. The three eigenvalues of D (λ_1, λ_2 , λ_3) represent the principal diffusivities along these main axes. They are sorted according to magnitude with λ_1 representing the highest and λ_3 representing the lowest diffusivity.

diffusion tensor displayed as an ellipsoid.

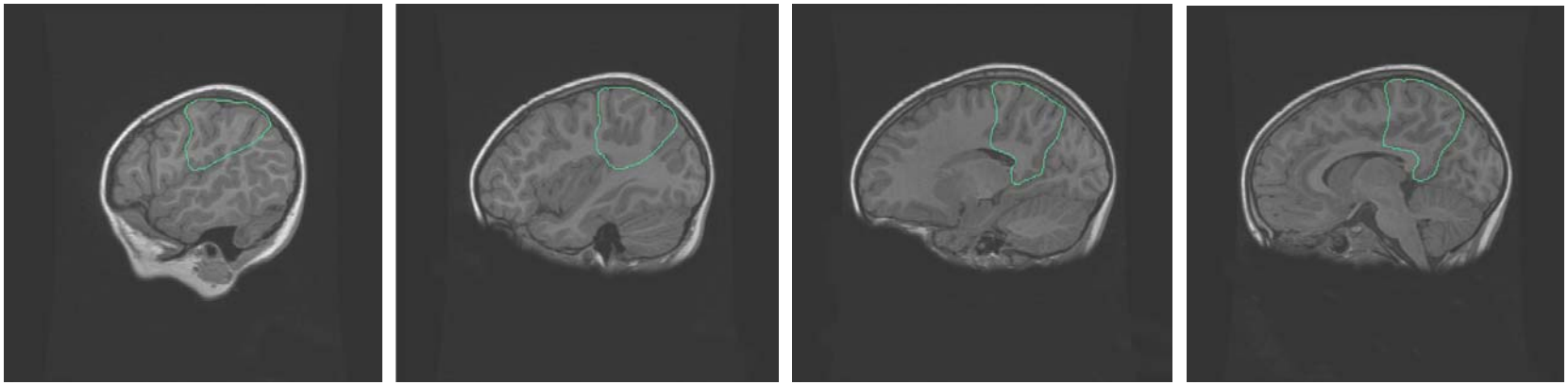

Figure 2a. Representative examples of region of interest (ROI) definition of the total parietal lobe and regional subdivisions on a high resolution T1-weighted image in a control participant

Figure 2a Continued

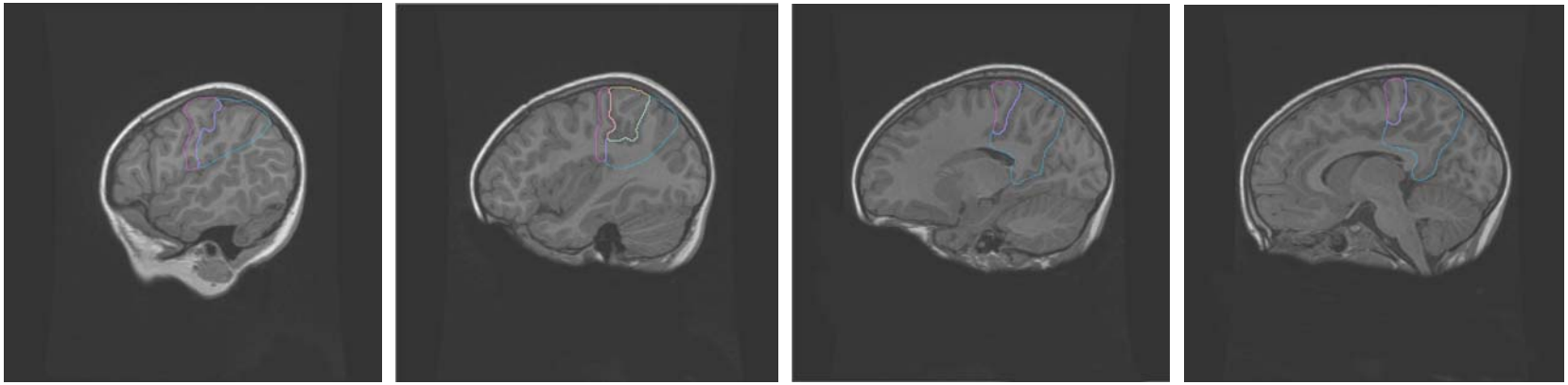

Note. Anterior-posterior outline of regions: postcentral gyrus (magenta-purple; magenta-orange); superior parietal lobule (orange-green); inferior temporal lobule (purple-blue; green-blue).

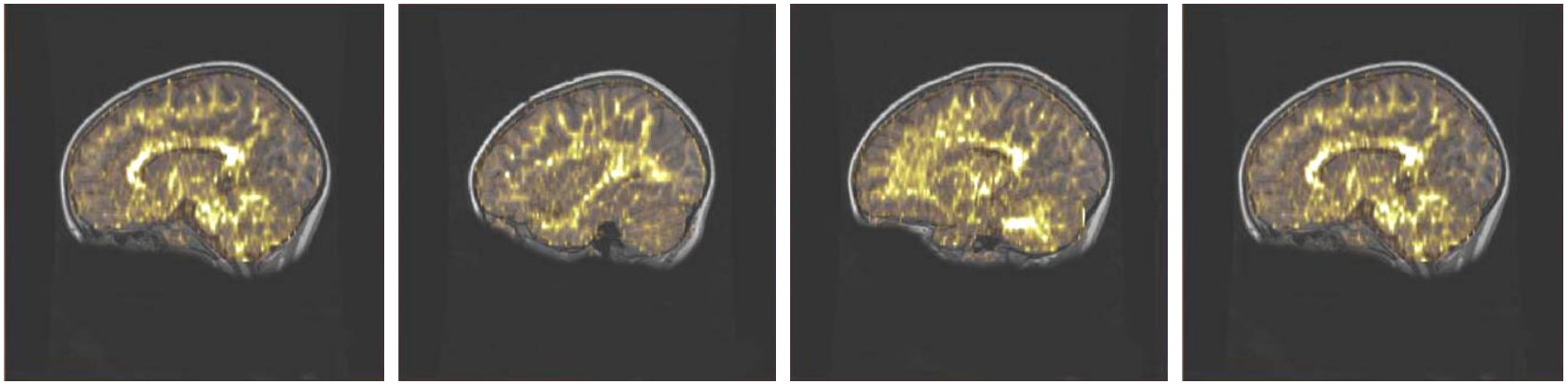

Figure 2b. Overlay of the fractional anisotropy (FA) map on the high resolution T1-weighted image

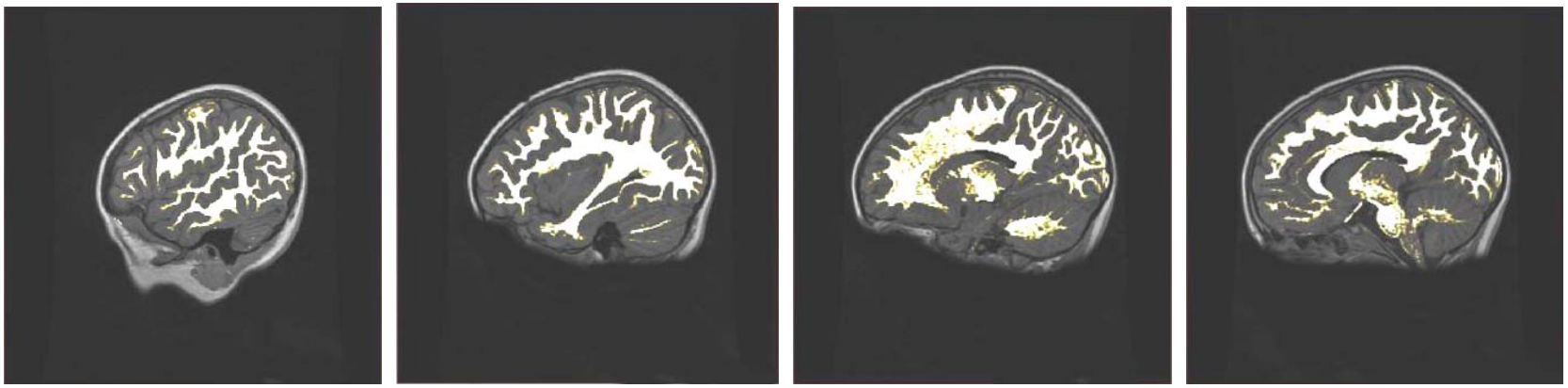

Figure 2c. Illustration of segmented white matter image used for extracting mean diffusion parameters from defined regions of interest

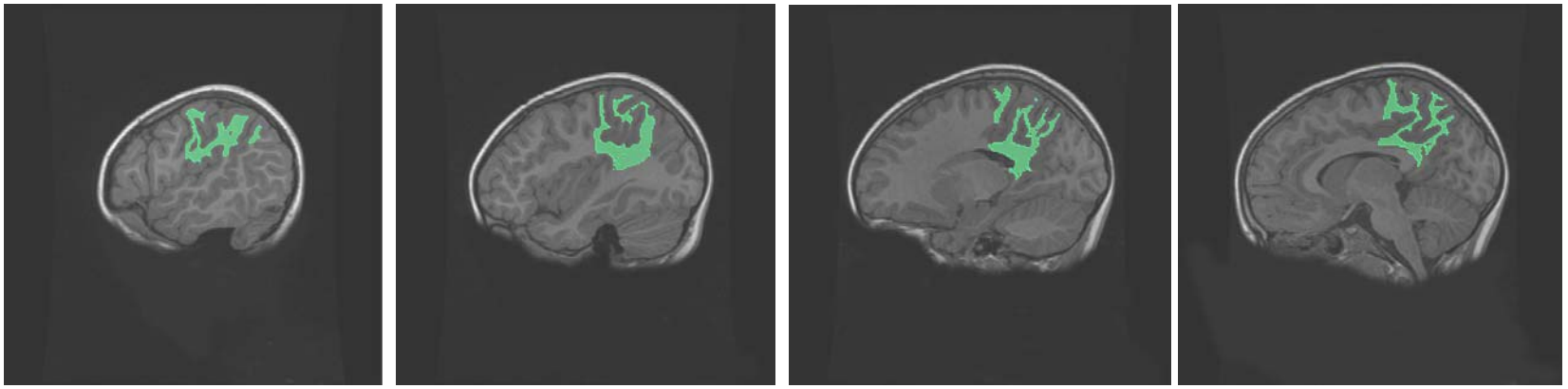

Figure 2d. Product of white matter segment and total parietal region of interest

Note. Images are presented in the Sagittal plane. Age of control participant is 5.5 years.

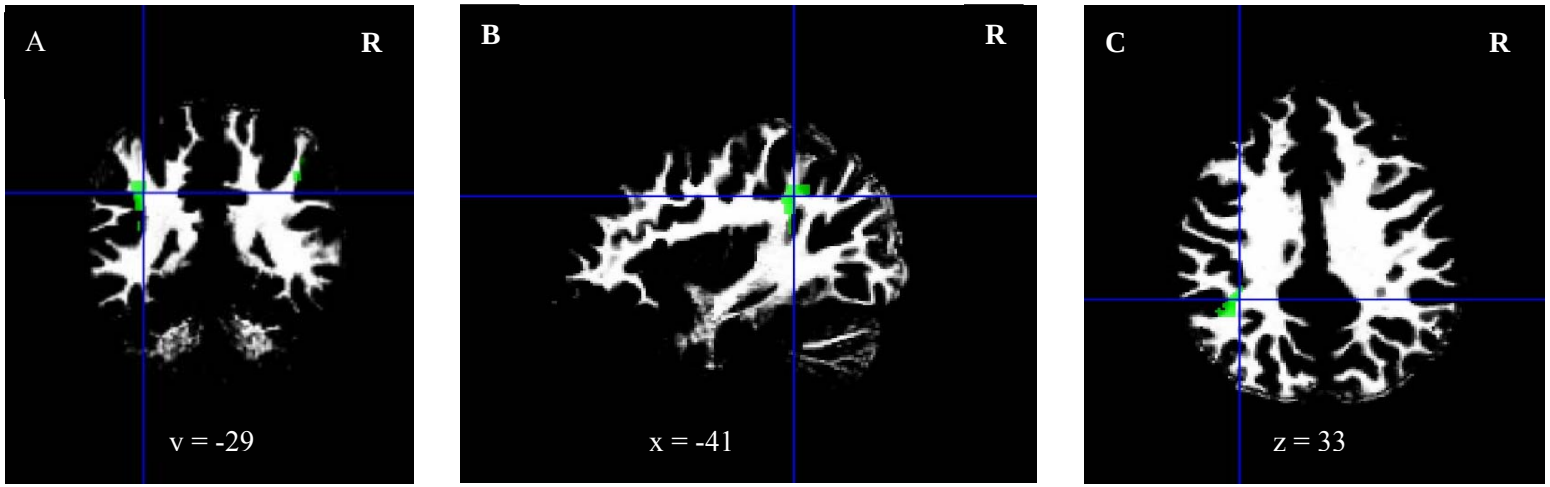

Figure 3. Coronal (A), sagittal (B), and transverse (C) views of voxels with a significant decrease in fractional anisotropy in the left inferior parietal lobule (global maximum with P =.03, corrected for entire cerebral volume; -29 -41 33 mm) in 24 children with cystinosis compared with controls. Results are superimposed on the white matter segment of a spatially normalized T1-weighted MRI.

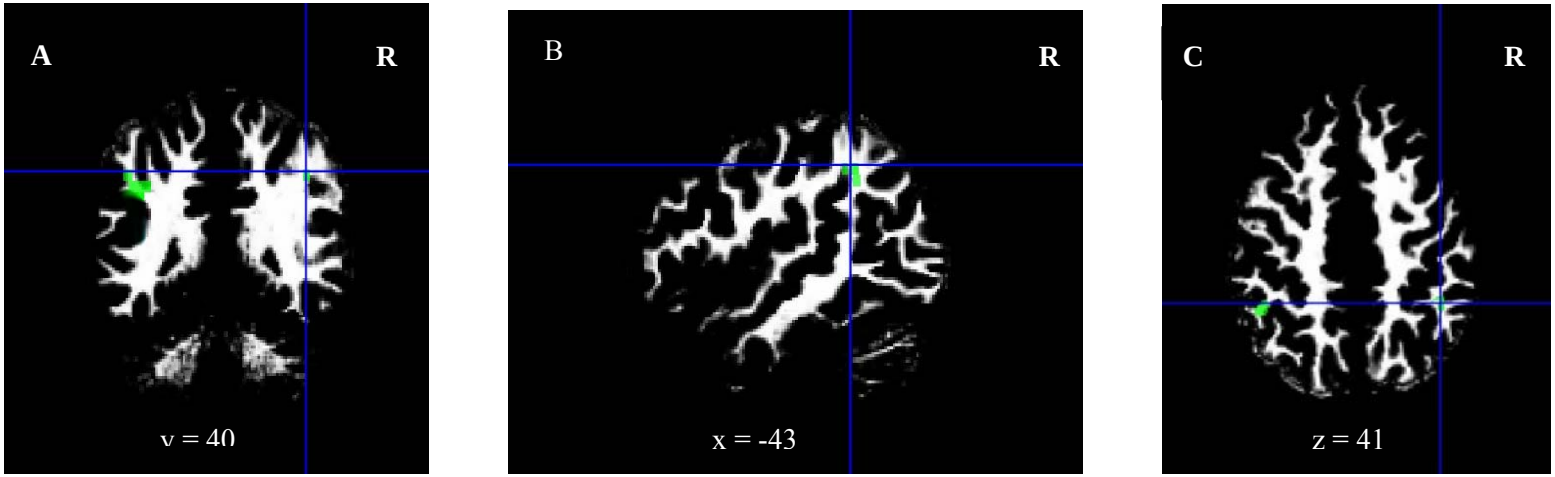

Figure 4. Coronal (A), sagittal (B), and transverse (C) views of voxels with a significant decrease in fractional anisotropy in the right superior parietal (P =.03, corrected for entire cerebral volume; 40 -43 41 mm) in 24 children with cystinosis compared with controls. Results are superimposed on the white matter segment of a spatially normalized T1-weighted MRI.

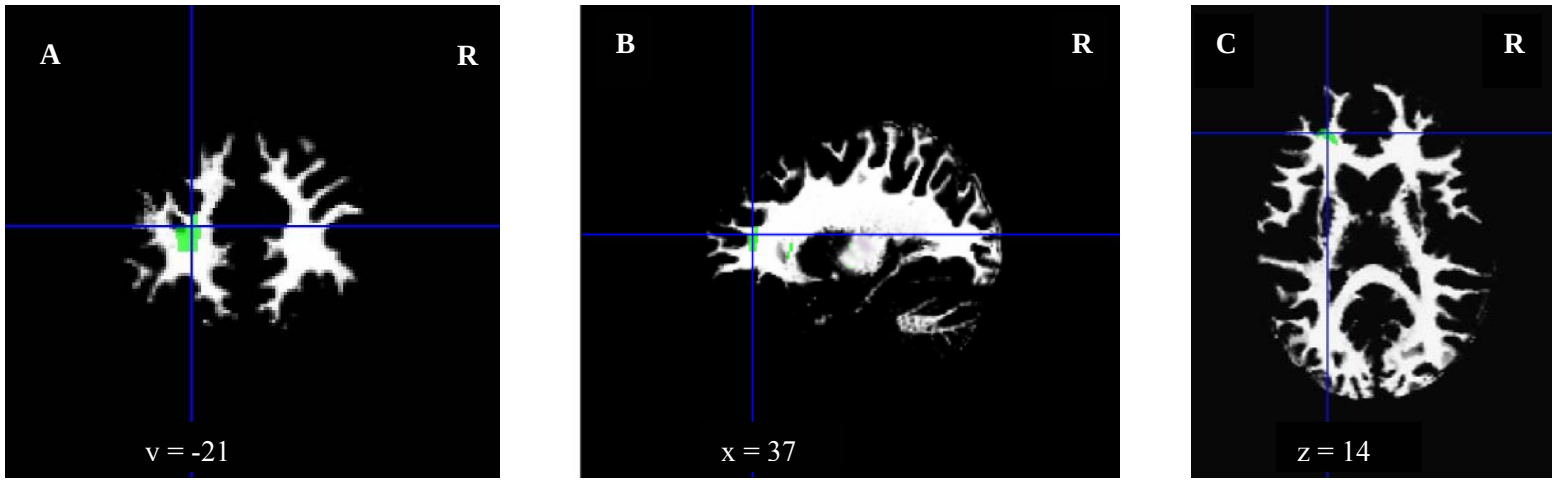

Figure 5. Coronal (A), sagittal (B), and transverse (C) views of voxels with a significant decrease in fractional anisotropy in the left superior frontal lobe (P =.03, corrected for entire cerebral volume; -21 37 14 mm) in 24 children with cystinosis compared with controls. Results are superimposed on the white matter segment of a spatially normalized T1-weighted MRI.

A.

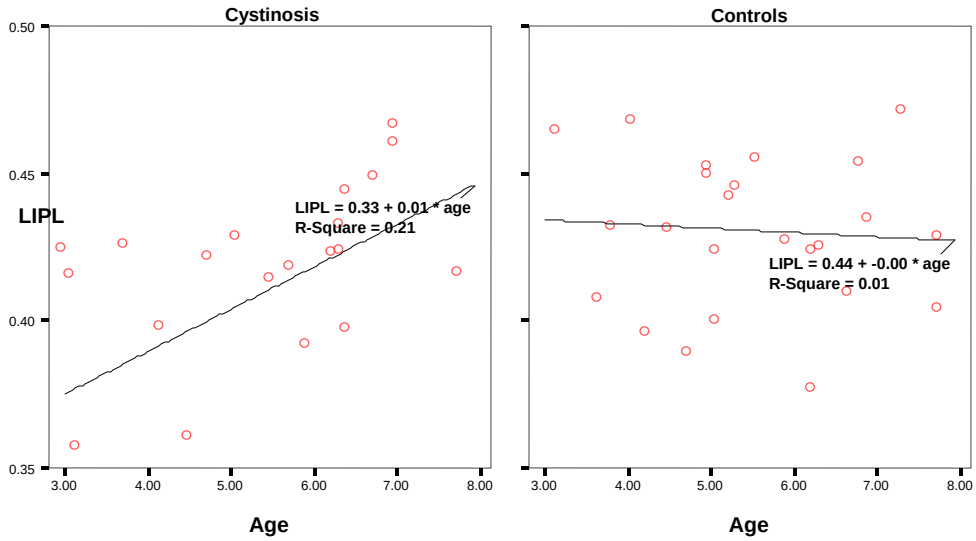

B.

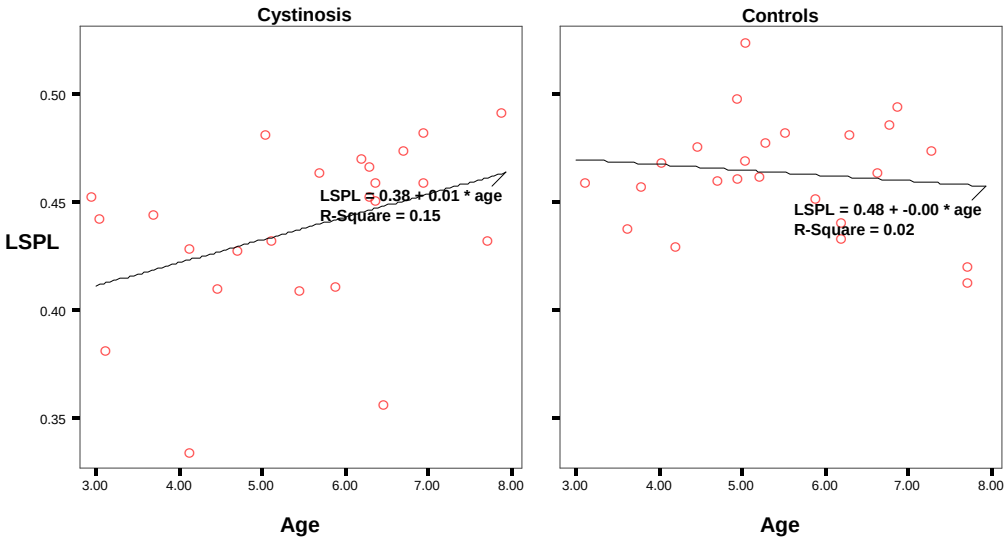

Figure 6. Scatterplots depicting the relationship between age and fractional anisotropy in in cystinosis and control participants. Regions include the (A) left inferior parietal lobule (LIPL), (B) left superior parietal lobule (LSPL), (C) right inferior parietal lobule (RIPL), and (D) right superior parietal lobule (RSPL).

Figure 6. Continued

C.

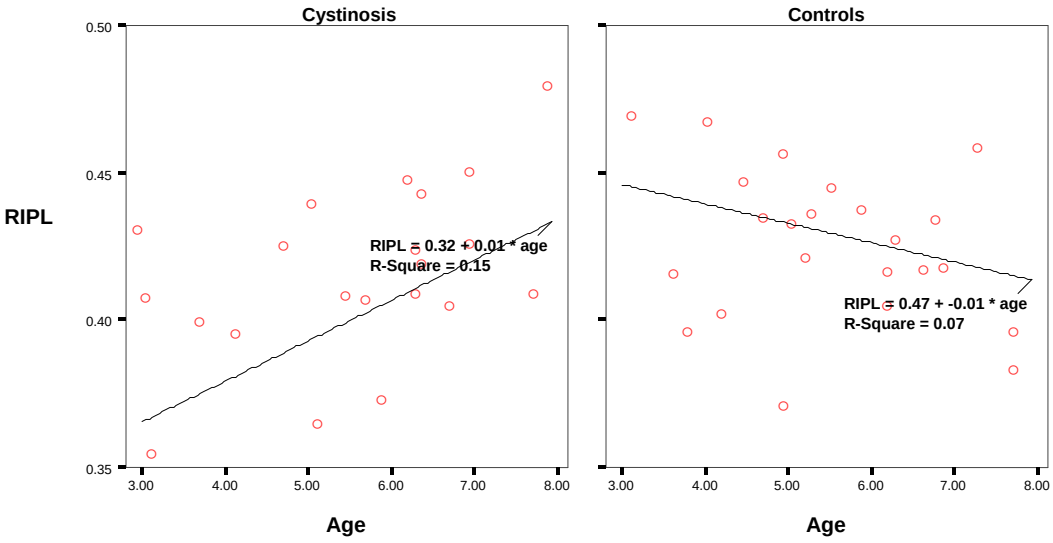

D.

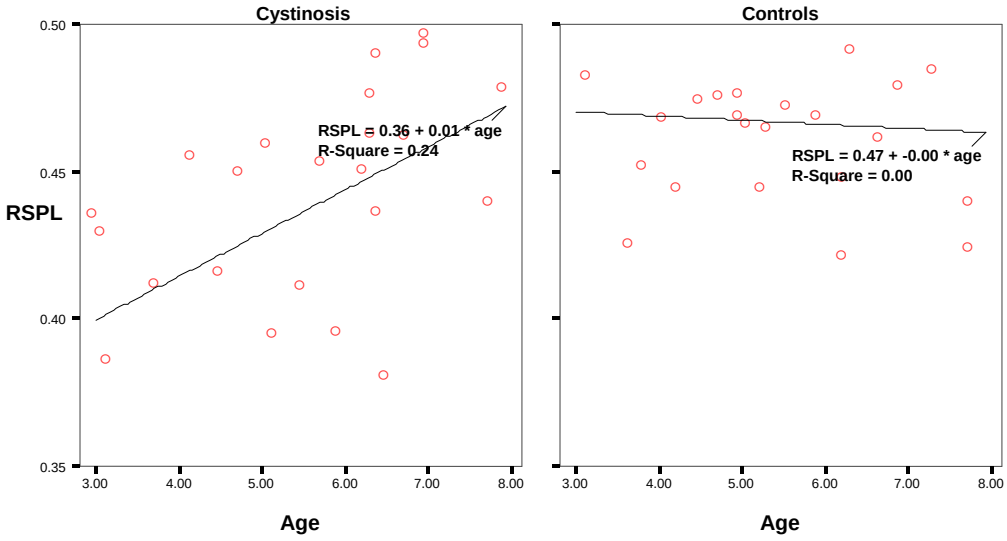

Table 1. Demographic characteristics and neuroradiological findings in children with cystinosis

Participant	Age*	Sex	Normal Clinical Reading	Volume Loss		Anomalies
				Cortical	Central	
1	3.00	F	Yes			
2	3.08	M	Yes			
3	3.17	F	No	Mild		
4	3.75	M	Yes			
5	4.17	M	No		Mild	
6	4.17	F	No			Chiari I malformation
7	4.50	M	No	Moderate	Moderate	
8	4.75	F	Yes			
9	5.08	F	No	Mild-Moderate	Mild-Moderate	
10	5.17	M	Yes			Cavum septum pellucidum & vergae (normal variant)
11	5.50	F	No	Mild		
12	5.75	M	No	Mild		
13	5.92	F	No	Moderate	Marked	
14	6.25	F	No	Mild	Mild	
15	6.33	M	Yes			
16	6.33	M	No			Right cerebellar tonsillar ectopia
17	6.42	F	Yes			
18	6.42	M	Yes			
19	6.50	M	Yes			
20	6.75	F	No			Borderline ventriculomegoly
21	7.00	F	No			Mild increase of superior vermian sulci
22	7.00	F	Yes			

Table 1 Continued

23	7.75	F	Yes
24	7.92	F	Yes

*Age in years
M = Male; F = Female

Table 2. Behavioral performance in cystinosis children and controls

	Cystinosis *(n = 24)*	Controls *(n = 24)*	T	*P*
Spatial Relations	103±10.8	116±8.5	4.6	.008*
VMI	89±12.0	107±15.9	4.0	.001*
PIQ	90±12.0	112±12.0	6.0	<.001*
VIQ	95±12.2	113±14.8	4.6	<.001*

*Significant at p = .05 with Hochberg correction for multiple comparisons

Table 3. Mean diffusion fractional anisotropy (FA) in cystinosis children and controls

	Cystinosis *(n = 24)*	Controls *(n = 24)*	F	*p*
LIPL	.41 ± .04	.43 ± .03	3.23	.079
LSPL	.44 ± .04	.46 ± .03	6.98	.011*
RIPL	.40 ± .05	.43 ± .03	5.71	.021*
RSPL	.44 ± .04	.47 ± .03	7.97	.007*
LITG	.38 ± .05	.38 ± .04	0.52	.476
RITG	.37 ± .05	.36 ± .04	0.02	.887

Abbreviations. L: Left; R: Right; IPL: inferior parietal lobule; SPL: superior parietal lobule; ITG: inferior temporal gyrus

*Significant at p = .05 with Hochberg correction for multiple comparisons

Table 4. Mean diffusivity (MD) in cystinosis children and controls

	Cystinosis *(n = 24)*	Controls *(n = 24)*	F	*p*
LIPL	.74 ± .08	.70 ± .04	2.97	.091
LSPL	.74 ± .08	.69 ± .03	3.95	.049*
RIPL	.73 ± .07	.70 ± .04	2.56	.117
RSPL	.75 ± .08	.70 ± .04	4.62	.037*
LITG	.72 ± .04	.72 ± .03	0.22	.643
RITG	.72 ± .03	.71 ± .05	1.10	.299

Abbreviations. L: Left; R: Right; IPL: inferior parietal lobule; SPL: superior parietal lobule; ITR: inferior temporal gyrus

*Significant at p = .05 with Hochberg correction for multiple comparisons

V. References

Aguirre, G. K., & D'Esposito, M. (1997). Environmental knowledge is subserved by separable dorsal/ventral neural areas. *J Neurosci, 17*(7), 2512-2518.

Alivisatos, B., & Petrides, M. (1997). Functional activation of the human brain during mental rotation. *Neuropsychologia, 35*(2), 111-118.

Anikster, Y., et al. (2001). Pulmonary dysfunction in adults with nephropathic cystinosis. *Chest, 119*(2), 394-401.

Ashburner, J., & Friston, K. J. (1997). Multimodal image coregistration and partitioning-a unified framework. *Neuroimage, 6*, 209-217.

Ballantyne, A. O., Scarvie, K. M., & Trauner, D. A. (1997). Academic achievement in individuals with infantile nephropathic cystinosis. *Am J Med Genet, 74*(2), 157-161.

Ballantyne, A. O., & Trauner, D. A. (2000). Neurobehavioral consequences of a genetic metabolic disorder: visual processing deficits in infantile nephropathic cystinosis. *Neuropsychiatry Neuropsychol Behav Neurol, 13*(4), 254-263.

Barnea-Goraly, N., et al. (2005). White Matter Development During Childhood and Adolescence: A Cross-sectional Diffusion Tensor Imaging Study. *Cereb Cortex*.

Basser, P. J., Mattiello, J., & LeBihan, D. (1994a). Estimation of the effective self-diffusion tensor from the NMR spin echo. *J Magn Reson B, 103*(3), 247-254.

Basser, P. J., Mattiello, J., & LeBihan, D. (1994b). MR diffusion tensor spectroscopy and imaging. *Biophys J, 66*(1), 259-267.

Baumann, N., & Pham-Dinh, D. (2001). Biology of oligodendrocyte and myelin in the mammalian central nervous system. *Physiol Rev, 81*(2), 871-927.

Beaulieu, C., & Allen, P. S. (1994). Water diffusion in the giant axon of the squid: implications for diffusion-weighted MRI of the nervous system. *Magn Reson Med, 32*(5), 579-583.

Beery, K.E., Buktenica, N.A., & Beery, N.A. (2004). Developmental Test of Visual Motor Integration (VMI) 5th Edition**,** Los Angeles: Western Psychological Services.

Boussaoud, D., di Pellegrino, G., & Wise, S. P. (1995). Frontal lobe mechanisms subserving vision-for-action versus vision-for-perception. *Behav Brain Res, 72*(1-2), 1-15.

Brody, B. A., Kinney, H. C., Kloman, A. S., & Gilles, F. H. (1987). Sequence of central nervous system myelination in human infancy. I. An autopsy study of myelination. *J Neuropathol Exp Neurol, 46*(3), 283-301.

Broyer, M., Tete, M. J., & Gubler, M. C. (1987). Late symptoms in infantile cystinosis. *Pediatr Nephrol, 1*(3), 519-524.

Broyer, M., et al. (1996). Clinical polymorphism of cystinosis encephalopathy. Results of treatment with cysteamine. *J Inherit Metab Dis, 19*(1), 65-75.

Butt, A. M., & Berry, M. (2000). Oligodendrocytes and the control of myelination in vivo: new insights from the rat anterior medullary velum. *J Neurosci Res, 59*(4), 477-488.

CCHMC pediatric brain template (2001). The Imaging Research Center. Cincinnati Childern's Hospital Medical Center. Retrieved, from the World Wide Web: http://www.irc.cchmc.org

Charnas, L. R., et al. (1994). Distal vacuolar myopathy in nephropathic cystinosis. *Ann Neurol, 35*(2), 181-188.

Cochat, P., Drachman, R., Gagnadoux, M. F., Pariente, D., & Broyer, M. (1986). Cerebral atrophy and nephropathic cystinosis. *Arch Dis Child, 61*(4), 401-403.

Cohen, M. S., et al. (1996). Changes in cortical activity during mental rotation. A mapping study using functional MRI. *Brain, 119 (Pt 1)*, 89-100.

Colah, S., & Trauner, D. A. (1997). Tactile recognition in infantile nephropathic cystinosis. *Dev Med Child Neurol, 39*(6), 409-413.

Colby, C. L., & Goldberg, M. E. (1999). Space and attention in parietal cortex. *Annu Rev Neurosci, 22*, 319-349.

Corballis, M. C. (1997). Mental rotation and the right hemisphere. *Brain Lang, 57*(1), 100-121.

Courtney, S. M., Ungerleider, L. G., Keil, K., & Haxby, J. V. (1996). Object and spatial visual working memory activate separate neural systems in human cortex. *Cereb Cortex, 6*(1), 39-49.

Cox RW (1996) AFNI: Software for analysis and visualization of functional magnetic resonance neuroimages. *Comput Biomed Res 29*,162–173.

Delgado, G., Schatz, A., Nichols, S., Appelbaum, M., & Trauner, D. (2005). Behavioral profiles of children with infantile nephropathic cystinosis. *Dev Med Child Neurol, 47*(6), 403-407.

DeYoe, E. A., & Van Essen, D. C. (1988). Concurrent processing streams in monkey visual cortex. *Trends Neurosci, 11*(5), 219-226.

Ditunno, P. L., & Mann, V. A. (1990). Right hemisphere specialization for mental rotation in normals and brain damaged subjects. *Cortex, 26*(2), 177-188.

Ebbesen, F., Mygind, K. I., & Holck, F. (1976). Infantile nephropatic cystinosis in Denmark. *Dan Med Bull, 23*(5), 216-222.

Ehrich, J. H., Stoeppler, L., Offner, G., & Brodehl, J. (1979). Evidence for cerebral involvement in nephropathic cystinosis. *Neuropadiatrie, 10*(2), 128-137.

Ehrich, J. H., et al. (1979). [Psychosocial intellectual development of children with infantile cystinosis and cerebral atrophy (author's transl)]. *Klin Padiatr, 191*(5), 483-492.

Feksa, L. R., et al. (2004). Inhibition of pyruvate kinase activity by cystine in brain cortex of rats. *Brain Res, 1012*(1-2), 93-100.

Filippi, C. G., et al. (2003). Diffusion-tensor MR imaging in children with developmental delay: preliminary findings. *Radiology, 229*(1), 44-50.

Fink, J. K., et al. (1989). Neurologic complications in long-standing nephropathic cystinosis. *Arch Neurol, 46*(5), 543-548.

Fivush, B., et al. (1987). Pancreatic endocrine insufficiency in posttransplant cystinosis. *Am J Dis Child, 141*(10), 1087-1089.

Friston, K. J., et al. (1995). Spatial registration and normalization of images. *Hum Brain Mapp, 3*, 165-189.

Gahl, W. A. (1986). Cystinosis coming of age. *Adv Pediatr, 33*, 95-126.

Gahl, W. A. (1995). Linkage of the gene for cystinosis to markers on the short arm of chromosome 17. The Cystinosis Collaborative Research Group. *Nat Genet, 10*(2), 246-248.

Gahl, W. A., et al. (1988). Myopathy and cystine storage in muscles in a patient with nephropathic cystinosis. *N Engl J Med, 319*(22), 1461-1464.

Gahl, W. A., et al. (1987). Cysteamine therapy for children with nephropathic cystinosis. *N Engl J Med, 316*(16), 971-977.

Gahl, W. A., Schneider, J. A., Thoene, J. G., & Chesney, R. (1986). Course of nephropathic cystinosis after age 10 years. *J Pediatr, 109*(4), 605-608.

Gahl, W. A., Thoene, J. G., & Schneider, J. A. (2001). Cystinosis: a disorder of lysosomal membrane transport. In B. A. Scriver CR, Valle D, Sly WS (Ed.), *The Metabolic and Molecular Bases of Inherited Diseases.* (8th ed., pp. 5085-5108). New York: McGraw-Hill.

Gahl, W. A., Thoene, J. G., & Schneider, J. A. (2002). Cystinosis. *N Engl J Med, 347*(2), 111-121.

Gieselmann, V., Polten, A., Kreysing, J., & von Figura, K. (1994). Molecular genetics of metachromatic leukodystrophy. *J Inherit Metab Dis, 17*(4), 500-509.

Goodale, M. A., & Milner, A. D. (1992). Separate visual pathways for perception and action. *Trends Neurosci, 15*(1), 20-25.

Hardy, R. J., & Friedrich, V. L., Jr. (1996). Progressive remodeling of the oligodendrocyte process arbor during myelinogenesis. *Dev Neurosci, 18*(4), 243-254.

Haxby, J. V., et al. (1994). The functional organization of human extrastriate cortex: a PET-rCBF study of selective attention to faces and locations. *J Neurosci, 14*(11 Pt 1), 6336-6353.

Hittmair, K., et al. (1994). MR assessment of brain maturation: comparison of sequences. *AJNR Am J Neuroradiol, 15*(3), 425-433.

Hodge, B. L., Hesselink, J. R., & Trauner, D. A. (1992). *Society for Neuroscience, 18*, 333.

Huppi, P. S., et al. (1998). Microstructural development of human newborn cerebral white matter assessed in vivo by diffusion tensor magnetic resonance imaging. *Pediatr Res, 44*(4), 584-590.

Huttenlocher J., Newcombe N., & Sandberg E.H. (1994). The coding of spatial location in young children. *Cognit Psychol*, *27*(2):115-47.

James, T. W., Culham, J., Humphrey, G. K., Milner, A. D., & Goodale, M. A. (2003). Ventral occipital lesions impair object recognition but not object-directed grasping: an fMRI study. *Brain, 126*(Pt 11), 2463-2475.

James, T. W., Humphrey, G. K., Gati, J. S., Menon, R. S., & Goodale, M. A. (2002). Differential effects of viewpoint on object-driven activation in dorsal and ventral streams. *Neuron, 35*(4), 793-801.

Jeannerod, M., & Jacob, P. (2005). Visual cognition: a new look at the two-visual systems model. *Neuropsychologia, 43*(2), 301-312.

Jelacic S, de Regt D, Weinberger E. (2006). Interactive digital MR atlas of the pediatric brain. R*adiographics*, *26*(2):497-501.

Jonas, A. J., et al. (1987). Nephropathic cystinosis with central nervous system involvement. *Am J Med, 83*(5), 966-970.

Jones D.K., Symms M.R., Cercignani M., & Howard R.J. (2005) The effect of filter size onVBM analyses of DT-MRI data. *Neuroimage, 26*(2):546-54.

Kaiser-Kupfer, M. I., Caruso, R. C., Minkler, D. S., & Gahl, W. A. (1986). Long-term ocular manifestations in nephropathic cystinosis. *Arch Ophthalmol, 104*(5), 706-711.

Keene, L. M. F., & Hewer, E. E. (1931). Some observations on myelination in the human central nervous system. *J Anat, 66*, 1-13.

Kim, J., Crespo-Facorro, B., Andreasen, N.C., O'Leary, D.S., Zhang, B., Haris, G., ,Magnotta, V. A. (2000). An MRI-Based parcellation method for the temporal lobe. *Neuroimage, 11*, 271-288.

Klingberg, T., Vaidya, C. J., Gabrieli, J. D., Moseley, M. E., & Hedehus, M. (1999). Myelination and organization of the frontal white matter in children: a diffusion tensor MRI study. *Neuroreport, 10*(13), 2817-2821.

Kosslyn, S. M., DiGirolamo, G. J., Thompson, W. L., & Alpert, N. M. (1998). Mental rotation of objects versus hands: neural mechanisms revealed by positron emission tomography. *Psychophysiology, 35*(2), 151-161.

Le Bihan, D., et al. (2001). Diffusion tensor imaging: concepts and applications. *J Magn Reson Imaging, 13*(4), 534-546.

Levine, S., & Paparo, G. (1982). Brain lesions in a case of cystinosis. *Acta Neuropathol (Berl), 57*(2-3), 217-220.

Mamata, H., et al. (2002). High-resolution line scan diffusion tensor MR imaging of white matter fiber tract anatomy. *AJNR Am J Neuroradiol, 23*(1), 67-75.

Markello, T. C., Bernardini, I. M., & Gahl, W. A. (1993). Improved renal function in children with cystinosis treated with cysteamine. *N Engl J Med, 328*(16), 1157-1162.

McGrew, K. S., & Woodcock, R. W. (1985). Woodcock-Johnson Psychoeducational Battery and Scales of Independent Behavior: Subtest Norms for the WJ/SIB Assessment System. U.S.A.: DLM Teaching Resources.

Mehta, Z., & Newcombe, F. (1991). A role for the left hemisphere in spatial processing. *Cortex, 27*(2), 153-167.

Moritani, T., Ekholm, S., & Westesson, P. (2004). *Diffusion-weighted MR imaging of the brain*. Berlin: Springer.

Morriss, M. C., Zimmerman, R. A., Bilaniuk, L. T., Hunter, J. V., & Haselgrove, J. C. (1999). Changes in brain water diffusion during childhood. *Neuroradiology, 41*(12), 929-934.

Mukherjee, P., et al. (2001). Normal brain maturation during childhood: developmental trends characterized with diffusion-tensor MR imaging. *Radiology, 221*(2), 349-358.

Mukherjee, P., et al. (2002). Diffusion-tensor MR imaging of gray and white matter development during normal human brain maturation. *AJNR Am J Neuroradiol, 23*(9), 1445-1456.

Mulligan, K.A., & Sundsten, Ph.D. (1998). Neuroanatomy interactive syllabus. University of Washington.

Neil, J. J., Miller, J., Mukherjee, P., & Huppi, P. S. (2002). Diffusion tensor imaging of normal and injured developing human brain - a technical review. *NMR Biomed, 15*(7-8), 543-552.

Neil, J. J., et al. (1998). Normal brain in human newborns: apparent diffusion coefficient and diffusion anisotropy measured by using diffusion tensor MR imaging. *Radiology, 209*(1), 57-66.

Nichols, S. L., Press, G. A., Schneider, J. A., & Trauner, D. A. (1990). Cortical atrophy and cognitive performance in infantile nephropathic cystinosis. *Pediatr Neurol, 6*(6), 379-381.

Nolte U.G., Finsterbusch J., & Frahm J. (2000). Rapid isotropic diffusion mapping without susceptibility artifacts: whole brain studies using diffusion-weighted single-shot STEAM MR imaging. *Magn Res Med 44*, 731-736.

Nomura, Y., et al. (1994). Diffusional anisotropy of the human brain assessed with diffusion-weighted MR: relation with normal brain development and aging. *AJNR Am J Neuroradiol, 15*(2), 231-238.

Oshima, R. G., Willis, R. C., Furlong, C. E., & Schneider, J. A. (1974). Binding assays for amino acids. The utilization of a cystine binding protein from Escherichia coli for the determination of acid-soluble cystine in small physiological samples. *J Biol Chem, 249*(19), 6033-6039.

Papachristou, D. N., Liu, J. L., & Patel, Y. C. (1994). Cysteamine-induced reduction in tissue somatostatin immunoreactivity is associated with alterations in somatostatin mRNA. *Regul Pept, 49*(3), 237-247.

Parsons, L. M., et al. (1995). Use of implicit motor imagery for visual shape discrimination as revealed by PET. *Nature, 375*(6526), 54-58.

Partridge, S. C., et al. (2004). Diffusion tensor imaging: serial quantitation of white matter tract maturity in premature newborns. *Neuroimage, 22*(3), 1302-1314.

Paus, T., et al. (2001). Maturation of white matter in the human brain: a review of magnetic resonance studies. *Brain Res Bull, 54*(3), 255-266.

Pierpaoli, C., & Basser, P. J. (1996). Toward a quantitative assessment of diffusion anisotropy. *Magn Reson Med, 36*(6), 893-906.

Pisoni, R. L., Thoene, J. G., & Christensen, H. N. (1985). Detection and characterization of carrier-mediated cationic amino acid transport in lysosomes of normal and cystinotic human fibroblasts. Role in therapeutic cystine removal? *J Biol Chem, 260*(8), 4791-4798.

Prayer, D., et al. (2001). Visualization of nonstructural changes in early white matter development on diffusion-weighted MR images: evidence supporting premyelination anisotropy. *AJNR Am J Neuroradiol, 22*(8), 1572-1576.

Rao, H., Zhou, T., Zhuo, Y., Fan, S., & Chen, L. (2003). Spatiotemporal activation of the two visual pathways in form discrimination and spatial location: a brain mapping study. *Hum Brain Mapp, 18*(2), 79-89.

Ross, D. L., Strife, C. F., Towbin, R., & Bove, K. E. (1982). Nonabsorptive hydrocephalus associated with nephropathic cystinosis. *Neurology, 32*(12), 1330-1334.

Sakuma, H., et al. (1991). Adult and neonatal human brain: diffusional anisotropy and myelination with diffusion-weighted MR imaging. *Radiology, 180*(1), 229-233.

Scarvie, K. M., Ballantyne, A. O., & Trauner, D. A. (1996). Visuomotor performance in children with infantile nephropathic cystinosis. *Percept Mot Skills, 82*(1), 67-75.

Schatz, A. (2002). Visual and verbal learning in a genetic metabolic disorder. *Dissertation Abstracts International: Section B: The Sciences & Engineering, 63 (4-B)*, 2073.

Schmithorst, V. J., Wilke, M., Dardzinski, B. J., & Holland, S. K. (2002). Correlation of white matter diffusivity and anisotropy with age during childhood and adolescence: a cross-sectional diffusion-tensor MR imaging study. *Radiology, 222*(1), 212-218.

Schmithorst, V. J., Wilke, M., Dardzinski, B. J., & Holland, S. K. (2005). Cognitive functions correlate with white matter architecture in a normal pediatric population: A diffusion tensor MRI study. *Hum Brain Mapp*, *26*(2), 139-47.

Schmithorst V.J., Holland S.K., & Dardzinski B.J. (2007). Developmental differences in white matter architecture between boys and girls. (in press) *Hum Brain Mapp*.

Schneider, J. A., Katz, B., & Melles, R. B. (1990). Update on nephropathic cystinosis. *Pediatr Nephrol, 4*(6), 645-653.

Shen, L., Hu, X., Yacoub, E., & Ugurbil, K. (1999). Neural correlates of visual form and visual spatial processing. *Hum Brain Mapp, 8*(1), 60-71.

Shimony, J. S., et al. (1999). Quantitative diffusion-tensor anisotropy brain MR imaging: normative human data and anatomic analysis. *Radiology, 212*(3), 770-784.

Smith, E.E. & Jonides, J. (1999). Storage and executive processes in the frontal lobes. *Science*, *283*(5408), 1657-61.

Smith, M., Furlong, C. E., Greene, A. A., & Schneider, J. A. (1987). Cystine: binding protein assay. *Methods Enzymol, 143*, 144-148.

Smolin, L. A., Clark, K. F., & Schneider, J. A. (1987). An improved method for heterozygote detection of cystinosis, using polymorphonuclear leukocytes. *Am J Hum Genet, 41*(2), 266-275.

Snook, L., Paulson, L. A., Roy, D., Phillips, L., & Beaulieu, C. (2005). Diffusion tensor imaging of neurodevelopment in children and young adults. *Neuroimage, 26*(4), 1164-1173.

Spilkin, A., Ballantyne, A.O., Babchuck, L.R., & Trauner, D.A. (2007). Non-verbal deficits in young children with a genetic metabolic disorder: WPPSI-III performance in cystinosis. *Am J Med Gen, 144B,* 444-447.

Stejskal, E. O., & Tanner, J. E. (1965). Spin diffusion measurements: spin-echoes in the presence of a time-dependent field gradient. *J Chem Phys, 42*, 288-292.

Stephanova, D. I. (2001). Myelin as longitudinal conductor: a multi-layered model of the myelinated human motor nerve fibre. *Biol Cybern, 84*(4), 301-308.

Suzuki, Y., Matsuzawa, H., Kwee, I. L., & Nakada, T. (2003). Absolute eigenvalue diffusion tensor analysis for human brain maturation. *NMR Biomed, 16*(5), 257-260.

Thomalla, G., et al. (2004). Diffusion tensor imaging detects early Wallerian degeneration of the pyramidal tract after ischemic stroke. *Neuroimage, 22*(4), 1767-1774.

Thomas, J. L., et al. (2000). Spatiotemporal development of oligodendrocytes in the embryonic brain. *J Neurosci Res, 59*(4), 471-476.

Touchman, J. W., et al. (2000). The genomic region encompassing the nephropathic cystinosis gene (CTNS): complete sequencing of a 200-kb segment and discovery of a novel gene within the common cystinosis-causing deletion. *Genome Res, 10*(2), 165-173.

Town, M., et al. (1998). A novel gene encoding an integral membrane protein is mutated in nephropathic cystinosis. *Nat Genet, 18*(4), 319-324.

Trauner, D., Chase, C., & Ballantyne, A. O. (1989). Patterns of visual memory dysfunction in children with cystinosis. *Ann Neurol, 26*, 436.

Trauner, D., Chase, C., Scheller, J., Katz, B., & Schneider, J. A. (1988). Neurologic and cognitive deficits in children with cystinosis. *J Pediatr, 112*(6), 912-914.

Trauner, D., Spilkin, A.M., Williams, J., & Babchuck, L. (accepted) Journal of Pediatrics.

Trauner, D., Williams, B. L., Hesselink, J. R., & Schneider, J. A. MRI abnormalities and cognitive dysfunction in nephropathic cystinosis.

Ungerleider, L. G., & Haxby, J. V. (1994). 'What' and 'where' in the human brain. *Curr Opin Neurobiol, 4*(2), 157-165.

Ungerleider, L. G., & Mishkin, M. (1982). Two cortical visual systems. In R. J. W. Mansfield (Ed.), *Analysis of visual behavior.* (pp. 549-586). Cambridge: MIT Press.

van der Knaap, M. S., Breiter, S. N., Naidu, S., Hart, A. A., & Valk, J. (1999). Defining and categorizing leukoencephalopathies of unknown origin: MR imaging approach. *Radiology, 213*(1), 121-133.

van der Knaap, M. S., & Valk, J. (1995). *Magentic Resonance of Myelin, Myelination, and Myelin Disorders* (2nd ed.). Berlin: Springer.

Vanrie, J., Beatse, E., Wagemans, J., Sunaert, S., & Van Hecke, P. (2002). Mental rotation versus invariant features in object perception from different viewpoints: an fMRI study. *Neuropsychologia, 40*(7), 917-930.

Virta, A., Barnett, A., & Pierpaoli, C. (1999). Visualizing and characterizing white matter fiber structure and architecture in the human pyramidal tract using diffusion tensor MRI. *Magn Reson Imaging, 17*(8), 1121-1133.

Vogel, D. G., et al. (1990). Central nervous system involvement in nephropathic cystinosis. *J Neuropathol Exp Neurol, 49*(6), 591-599.

Wechsler, D. (1989). Wechsler Preschool and Primary Scale of Intelligence - Revised (WPPSI-R). San Antonio, (TX): Psychological Corporation.

Wechsler, D. (1991). Wechsler Intelligence Scale for Children - III (WISC-III). San Antonio, (TX): Psychological Corporation.

Wilke, M., Schmithorst, V. J., & Holland, S. K. (2003). Normative pediatric brain data for spatial normalization and segmentation differs from standard adult data. *Magn Reson Med, 50*(4), 749-757.

Williams, B. L., Schneider, J. A., & Trauner, D. A. (1994). Global intellectual deficits in cystinosis. *Am J Med Genet, 49*(1), 83-87.

Wimberger, D. M., et al. (1995). Identification of "premyelination" by diffusion-weighted MRI. *J Comput Assist Tomogr, 19*(1), 28-33.

Wolff, G., Ehrich, J. H., Offner, G., & Brodehl, J. (1982). Psychosocial and intellectual development in 12 patients with infantile nephropathic cystinosis. *Acta Paediatr Scand, 71*(6), 1007-1011.

Yakovlev, P. I., & Lecours, A. R. (1967). The myelogenetic cyscles of regional maturation of the brain. In A. Minowski (Ed.), *Regional development of the brain in early life* (pp. 3-70). Oxford: Blackwell.